

Spatial patterns of cadmium and lead deposition on and adjacent to National Park Service lands near Red Dog Mine, Alaska: NPS Final Report

Linda Hasselbach, Jay Ver Hoef, Jesse Ford, Peter Neitlich, Eric Crecelius, Shanti Berryman, Brett Wolk and Todd Bohle

Resource Report, NPS / AR / NRTR-2004-45

July 2004

United States Department of the Interior
National Park Service
Alaska Region
WEAR – Cape Krusenstern National Monument



The National Park Service, Alaska Region

Natural Resource Reports

The Alaska Region of the National Park Service manages 16 areas in Alaska. The diversity of areas and of their resources is reflected in their designation as national parks, monuments, preserves, and historical parks. These 16 areas represent more than 50 percent of the total acreage the National Park Service administers. The Alaska Region's Resource Management Program directs scientific research and resource management programs in a wide range of biological, physical, and social science disciplines.

The National Park Service disseminates reports on high priority, current resource management information, with managerial application, through the Alaska Region's Natural Resource Report Series. Technologies and resource management methods, resource management papers, proceedings of conferences and resource management workshops, and natural resource management plans are also disseminated through this series. Documents in this series usually contain information prepared primarily for internal use by the National Park Service.

Mention of trade names or commercial products does not constitute endorsement or recommendation for use by the National Park Service.

To order a copy from the National Park Service, use the reference number on the report's title page. Copies of this report are available online at www/nps.gov/akso/NPS_CAKR-Metals_2004.pdf or from the following:

National Park Service
P.O. Box 1029
Kotzebue, AK 99752
USA
Tel. 907/442-3890

Authors

L. Hasselbach¹, J. M. Ver Hoef², J. Ford³, P. Neitlich¹, E. Crecelius⁴, S. Berryman⁵, B. Wolk⁵ and T. Bohle⁶

¹National Park Service, PO Box 1029, Kotzebue, AK 99752, USA; Tel. 509 996 3203; E-mail: linda_hasselbach@nps.gov

²Alaska Department of Fish and Game, 1300 College Road, Fairbanks, AK 99701 USA

³Department of Fisheries and Wildlife, 104 Nash Hall, Oregon State University, Corvallis, OR 97331-3803, USA

⁴Battelle Marine Sciences Lab, 1529 West Sequim Bay Road, Sequim, WA 98382-9099, USA

⁵Department of Botany and Plant Pathology, Cordley Hall, Oregon State University, Corvallis, OR 97331, USA

⁶252 Xerxes Street, Minneapolis, MN 55405, USA

ABSTRACT

Heavy metal escapement associated with ore trucks is known to occur along the DeLong Mountain Regional Transportation System (DMTS) haul road corridor in Cape Krusenstern National Monument, northwest Alaska. Heavy metal concentrations in *Hylocomium splendens* moss ($n = 226$) were used in geostatistical models to predict the extent and pattern of airborne deposition of Cd and Pb on Monument lands. A stratified grid-based sample design was used with more intensive sampling near mine-related activity areas. Spatial predictions were used to produce maps of concentration patterns, and to estimate the total area in ten moss concentration categories.

Heavy metal levels in moss were highest immediately adjacent to the DMTS haul road (Cd > 24 mg/kg dw; Pb > 900 mg/kg dw). Spatial regression analyses indicated that heavy metal deposition decreased with the log of distance from the DMTS haul road and the DMTS port site. Analysis of subsurface soil suggested that observed patterns of heavy metal deposition reflected in moss were not attributable to subsurface lithology at the sample points. Further, moss Pb concentrations throughout the northern half of the study area were high relative to concentrations previously reported from other Arctic Alaska sites. Collectively, these findings indicate the presence of mine-related heavy metal deposition throughout the northern portion of Cape Krusenstern National Monument.

Geospatial analyses suggest that the Pb depositional area extends 25 km north of the haul road to the Kisimilot/Iyikrok hills, and possibly beyond. More study is needed to determine whether higher moss heavy metal concentrations in the northernmost portion of the study area reflect deposition from mining-related activities, weathering from mineralized Pb/Zn outcrops in the broader region, or a combination of the two. South of the DMTS haul road, airborne deposition appears to be constrained by the Tahinichok Mountains. Heavy metal levels continue to decrease south of the mountains, reaching a minimum in the southernmost portion of the study area near the Igichuk Hills (45 km from the haul road). The influence of the mine site was not studied.

CONTENTS

Abstract..... i

List of Tables iii

List of Figures..... iv

Introduction..... 1

Study Area 2

Methods..... 4

 Sample Design 4

 Sample Collection..... 7

 Quality Assurance (QA) in the Field 8

 Laboratory Work..... 8

 Spatial Analysis 9

Results..... 14

 Summary Data 14

 Elemental Correlations in Moss..... 15

 Spatial Regression..... 15

 Patterns of Heavy Metal Deposition..... 17

 Subsurface Soils..... 24

 Regional Context 24

 Geographic Extent of Deposition..... 27

Discussion..... 27

 Sources of Heavy Metal Escapement 27

 Heavy Metals and Dust..... 29

 Topography and Wind as Related to Moss Concentrations..... 30

 Extent of Depositional Area..... 31

Conclusions..... 33

Acknowledgements..... 35

References..... 36

Appendix I: Moss Data 42

Appendix II: Soil Data 49

Appendix III: Site Data..... 52

LIST OF TABLES

Table 1. Information on stratified sampling design based on random samples within a grid of cells.

Table 2. The number of points sampled for *Hylocomium splendens* by strata.

Table 3. Summary data for analytes in moss and subsurface soil throughout the entire study area, including median, mean, standard deviation (SD) and range of values.

Table 4. All pairwise correlation coefficients among element concentrations in *Hylocomium splendens* moss ($n = 151$).

Table 5. Spatial regression results examining relationships between moss concentrations and potential sources of airborne deposition across the entire study area.

Table 6. Comparison of Cd concentrations in *Hylocomium splendens* moss in the current study area with Arctic Alaska values reported by Ford et al. (1995).

Table 7. Comparison of Pb concentrations in *Hylocomium splendens* moss in the current study area with Arctic Alaska values reported by Ford et al. (1995).

Table 8. Conditional simulation estimates of heavy metal depositional areas within the study area and within Cape Krusenstern National Monument (NPS lands).

LIST OF FIGURES

Figure 1. Location map. Cape Krusenstern National Monument, Alaska.

Figure 2. Sample collection locations and strata definition.

Figure 3. Elemental concentrations in moss and subsurface soil with respect to the DMTS haul road.

Figure 4. Conditional simulation predictions for moss Cd concentrations in the vicinity of Cape Krusenstern National Monument including 0.05 and 0.95 prediction quantiles.

Figure 5. Conditional simulation predictions for moss Pb concentrations in the vicinity of Cape Krusenstern National Monument including 0.05 and 0.95 prediction quantiles.

Figure 6. Conditional simulation predictions for moss Pb concentrations along the DMTS haul road corridor.

Figure 7. Moss Pb concentration contours (derived from conditional simulation) overlain on topography in the vicinity of Cape Krusenstern National Monument. Inlay shows actual Pb concentrations in the northern portion of the study area.

INTRODUCTION

Cape Krusenstern National Monument is located in a remote region of northwestern Alaska and administered by the National Park Service (NPS). Neighboring Iñupiat village residents use Monument land for subsistence hunting and food-gathering activities. The largest zinc mine in the world, Red Dog Mine, is located approximately 50 km northeast of the Monument boundary. Since its inception in 1989, Red Dog Mine has operated year-round to produce lead (Pb) and zinc (Zn) concentrates in powder form at the mine site. Ore concentrates are hauled ca. 75 km in covered trucks via the DeLong Mountain Regional Transportation System (DMTS) haul road to storage facilities on the Chukchi Sea, where they are stored for further transport during the short ice-free shipping season.

The DMTS haul road (hereafter referred to as “haul road”) traverses 32 km of Monument land. In 1985, a 100-year transportation easement was granted for construction and use of the haul road through NPS land (Public Law 99-96, 1985). In 2001, NPS researchers reported high concentrations of cadmium (Cd >10 mg/kg), Pb (> 400 mg/kg), and Zn (> 1500 mg/kg) in and on *Hylocomium splendens* moss along the haul road corridor (Ford and Hasselbach 2001). The source of these high concentrations was attributed to escapement of ore concentrate from trucks and truck surfaces during transport (Ford and Hasselbach 2001). Sampling was concentrated near the haul road and no attempt was made to determine the extent of the depositional area. These findings formed the basis for the present study, which was designed to estimate the geographic extent and distribution patterns of heavy metal deposition within the Monument.

The NPS is required by law to protect natural and healthy ecosystems (Public Law 96-487, 1980). The ecosystem effects of artificially elevated Cd and Pb levels on Monument land are unknown at this time. Mining company consultants are currently conducting an extensive risk assessment effort under the oversight of the State of Alaska Department of Environmental Conservation. Information obtained through the current study will allow focused design of further studies the appropriate spatial scale. Follow-up research,

including determination of potential biological effects, can then be targeted in areas of greatest potential concern.

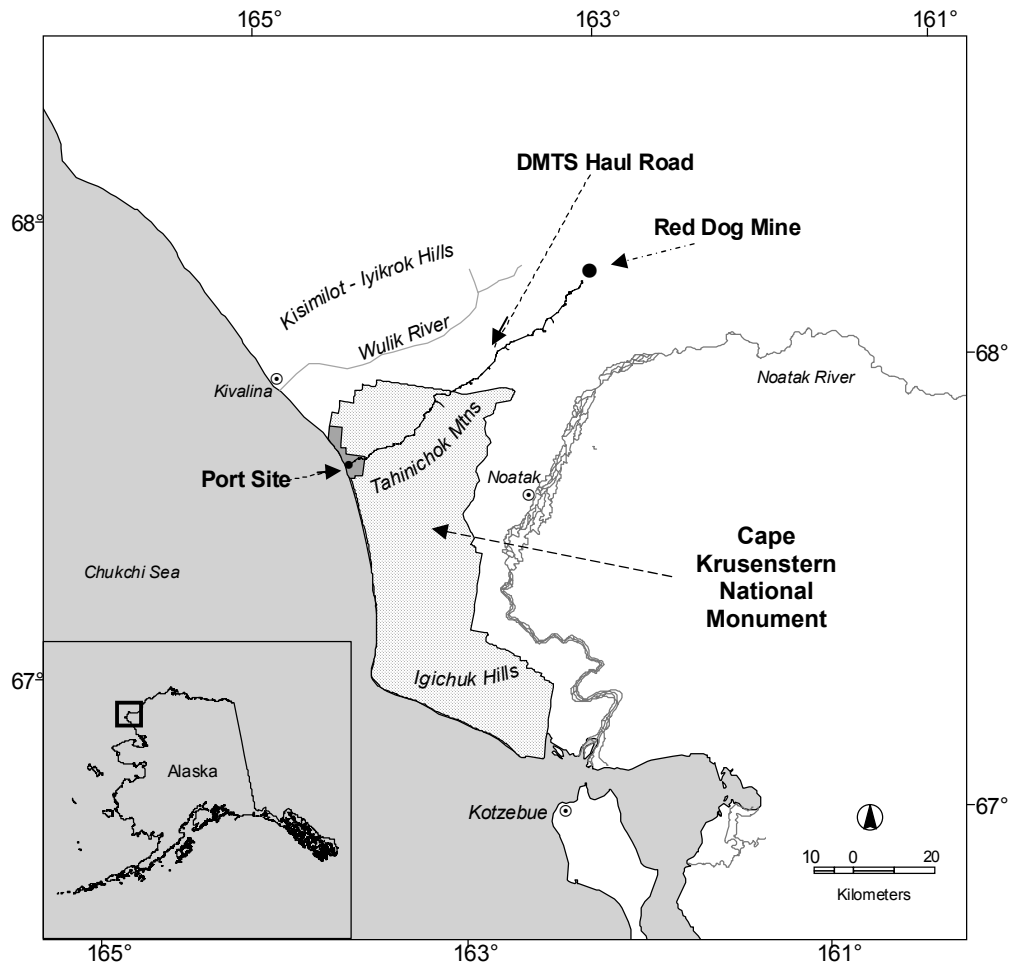
The use of *H. splendens* moss in assessing airborne contaminants is well established (e.g., Berg et al. 2003, Rühling and Steinnes 1998, Berg & Steinnes 1997, Steinnes 1995, Steinnes et al. 1992). Mosses lack vascular systems and obtain most of their nutrients from precipitation and from dry deposition of airborne particles (Aberg et al. 2001; Rühling and Steinnes 1998). Therefore, tissue concentrations are minimally confounded by uptake of mineral elements from soils and subsequent translocation. *H. splendens* has been particularly well characterized with respect to element uptake (e.g., Rühling and Tyler 1970), field variability (Ford et al. 1995, Økland 1999), and the relationship between tissue concentration and atmospheric deposition (Berg et al. 2003, Berg and Steinnes 1997, Ross 1990).

The goals of this study were: (1) to model the spatial patterns of atmospherically derived Cd and Pb deposition in the vicinity of Cape Krusenstern National Monument, (2) to estimate the areal extent of land with moss levels in various concentration categories, and (3) to identify potential sources of these airborne heavy metals.

STUDY AREA

Cape Krusenstern National Monument encompasses 266,700 ha bordering the Chukchi Sea approximately 16 km north of Kotzebue, Alaska (Figure 1). The Monument is located in a tundra ecosystem on a coastal plain with predominantly open low mixed shrub-sedge tussock tundra (Viereck et al. 1992) interspersed with low-lying, well-drained knolls supporting a variety of lichen, forb, and shrub species. Bedrock is predominantly calcareous and of Paleozoic age. Soils are poorly developed due to the cold climate, low precipitation, and the near-continuous permafrost.

Figure 1. Location map. Cape Krusenstern National Monument, Alaska.



The haul road bisects the northern portion of the Monument. Immediately south of the haul road, the Tahinichok Mountains are a dominant feature rising from the flat tussock tundra to a maximum elevation of 502 m. South of this mountain range, Monument lands are predominantly wet, flat, and rolling. The area north of the haul road is generally low-lying and gently sloping, and drains into the Wulik River approximately 10 km north of the Monument boundary.

The port facility (Figure 1) is located on land belonging to NANA Regional Corporation (an Alaska Native corporation) at the western terminus of the haul road. The facility itself is owned by the Alaska Industrial Development and Export Authority which

contracts with the mining company, Teck Cominco Alaska, Inc., for its use, operation and maintenance (Exponent 2002a).

Wind patterns throughout the study area are variable and are influenced by local topography (Exponent 2002b). Winds at the port site are typically from the northeast in winter months. In summer, port site winds are highly variable and strong winds from the south-southwest are present (Exponent 2002b). At the mine site, winds are predominantly from the northeast and southeast in winter months and highly variable in summer months (Exponent 2002b).

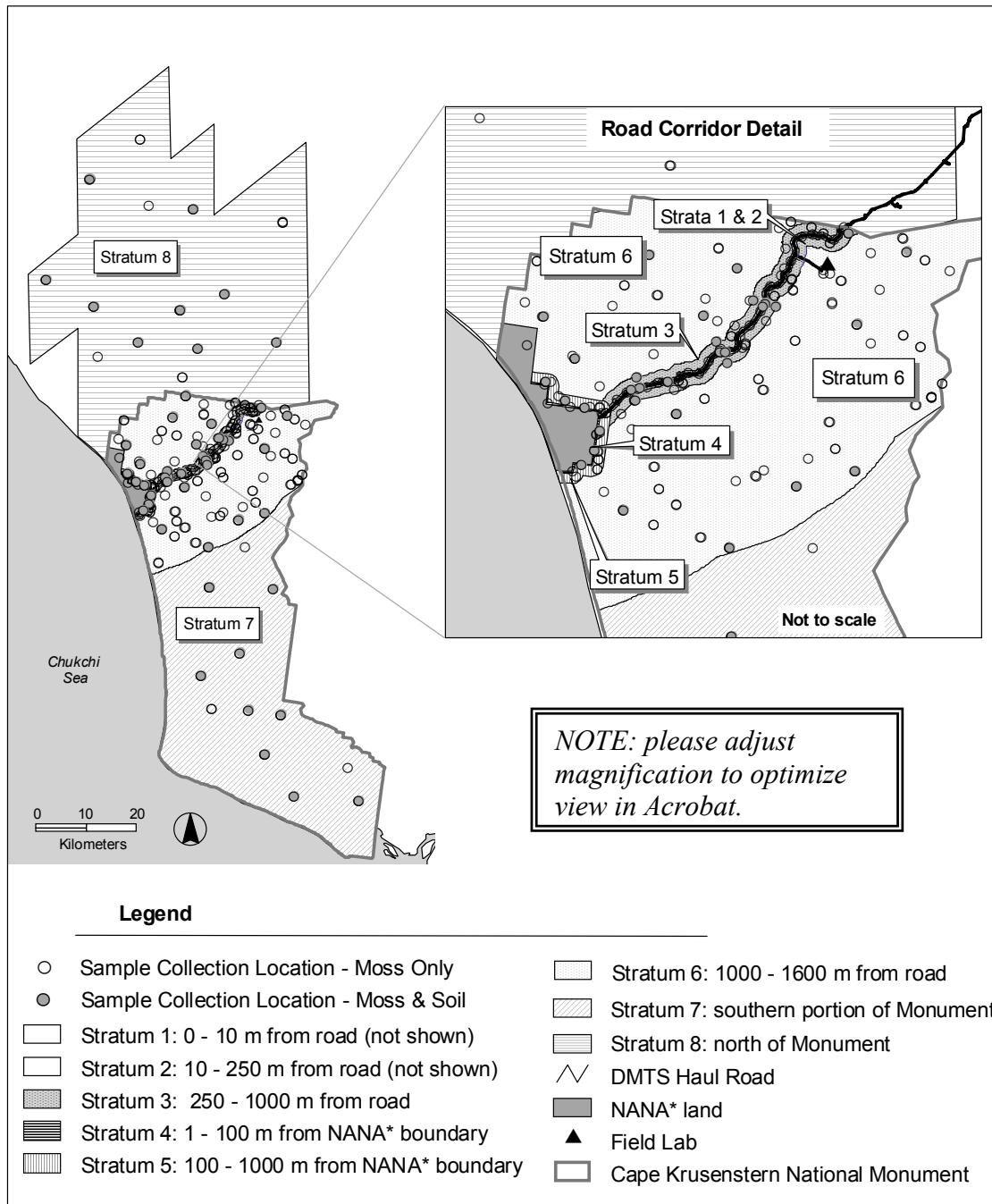
METHODS

Samples of the *H. splendens* moss and subsurface soil were collected from June through August 2001 in a 5000 km² area encompassing the Monument and lands to the north (Figure 2). The study area was centered on the portion of the haul road that crosses Monument lands, and extended approximately 70 km north and 70 km south of the road. Laboratory analysis targeted heavy metals of potential toxicological interest (Cd and Pb). Crustal elements (Al and Fe) and Zn were included for interpretive purposes.

Sample Design

A stratified, grid-based sample design was used with intensified sampling (i.e., smaller grid cell size) near the haul road and port site boundary. The grid consisted of 8 strata (Figure 2, Table 1) and a total of 155 grid cells (Table 2). Grid cell size increased gradually (by strata) with distance from the haul road and the port site, allowing for more intensive sampling (i.e., smaller and more numerous grid cells) near these features (Figure 2). The grid configuration was based on roadside deposition patterns revealed in pilot study data (Ford and Hasselbach 2001), as well as on time and budgetary considerations.

Figure 2. Sample collection locations and strata definition. Mosses were collected and analyzed at each grid cell location ($n = 151$). Subsurface soil collection locations are shown only for soils used in data analysis ($n = 46$).



* Northwest Arctic Native Association

Table 1. Information on stratified sampling design based on random samples within a grid of cells.

Stratum	Stratum Definition	Approximate Cell Size (km ²)
1	0 – 10 m from haul road	0.05
2	10 – 250 m from haul road	1
3	250 – 1000 m from haul road	3
4	0 – 100 m from NANA* port site boundary	0.20
5	100 – 1000 m from NANA* port site boundary	2
6	1000 – 16000 m from haul road	18
7	Southern portion of Monument (> 16000 m south of haul road)	200
8	North of Monument boundary (> 16000 m north of haul road)	200

* NANA Regional Corporation

Table 2. The number of points sampled for *Hylocomium splendens* by strata.

Stratum	Grid Cells Sampled	Grid Cells Unsampled*	Total Moss Collections**	Soil Collections***
1	12	0	13	5
2	13	0	15	2
3	18	2	30	1
4	8	0	9	3
5	8	0	13	3
6	66	1	103	13
7	12	0	19	9
8	14	1	24	10
Totals	151	4	227	46

* Not sampled due either to lack of moss or weather-related helicopter constraints.

** Including field duplicate and random duplicate collections.

*** Including only the subset of samples used for data analysis.

One primary and several auxiliary sample points were randomly chosen within each grid cell prior to field sampling. If a primary sample point did not contain sufficient *Hylocomium* (e.g., the sample point fell in a lagoon), an auxiliary point within the same grid cell was located and sampled. Data sheets were completed for all primary points, whether or not moss was present.

A single moss sample was collected at each sampling point. In addition, at 40% of the points, a second moss sample was collected in a random direction and distance (< 99 m) from the original point to enable estimates of short-range spatial correlations. These samples were referred to as “random duplicates.” Also, in 9% (i.e., 13) of the grid cells, an additional moss collection was made as close as possible to the original sampling point. These samples were designated as ‘field duplicates’ and were used to assist in the estimation of variance. Grid cells for collection of random duplicates and field duplicates were randomly selected prior to field sampling.

Mosses were collected on a total of 151 (out of 155) grid cells (Figure 2, Table 2). The grand total of 227 grid-based moss samples included 13 field duplicate and 62 random duplicate collections.

Sample Collection

Moss collection methods were identical to those used in Ford and Hasselbach (2001) and Ford et al. (1995). Unwashed moss samples were picked clean of visible debris (e.g., roots, pebbles) and cropped to include only the most recent (ca. 3–4 yrs) growth. Specimens were then air-dried on-site in a separate drying tent, sealed, and shipped to the analytical laboratory.

Samples of subsurface soils (mean collection depth = 62 cm) were obtained at each primary sample point. At 47 out of 151 points, we were unable to drill deeply enough through permafrost to obtain samples devoid of obvious organic material. Samples at depth that contained conspicuous organic material were not considered representative of soil parent material and were subsequently removed from the sample pool. Due to

funding constraints, only a subset of the remaining soil samples was sent for laboratory analysis ($n = 46$). These soils were selected randomly by stratum and were chosen so that all strata were represented (Figure 2, Table 2). Additional details on soil collection methodology are provided in Ford and Hasselbach (2001).

Quality Assurance (QA) in the Field

All samples were cleaned, dried in a dedicated drying tent, and packaged for transport at the on-site field laboratory (Figure 2). To assess ambient levels of heavy metals in the air at the laboratory site (potentially generated by both moss cleaning activity and haul road proximity), four sterile filters were placed in the field laboratory for 24 hours during a typical moss cleaning session. The same protocol was followed in the drying tent. One unexposed blank was also assigned for each session. All filters were analyzed for heavy metals and crustal elements. Results showed elemental content was below the reporting/quantitation limit of $3.18 \times \text{MDL}$ (Method Detection Limit), and so laboratory results for moss samples did not require correction for this potential source of contamination.

To verify moss identification and 3–5 year clipping accuracy, blind quality assurance checks were performed by the crew leader on 30% of all cleaned samples. Vouchers were retained for each moss sample.

Laboratory Work

Moss

Mosses were not washed as the intent was to study the sum of dry deposition + tissue concentrations in order to (1) capture the entirety of environmental contributions of heavy metals and (2) allow comparisons to previous studies. A ca. 300-mg aliquot of each dried sample was combined with nitric, hydrochloric, and hydrofluoric acids in a Teflon bomb and heated overnight in an oven at 130°C ($\pm 10^{\circ}\text{C}$). Acids were then neutralized with a boric acid solution by heating for four hours at 130°C (Shaole et al. 1996). Samples were brought up to volume with deionized water. Aluminum, Fe, and Zn were analyzed by inductively coupled plasma atomic emission spectrometry (ICP-AES); Cd and Pb were

analyzed by inductively coupled plasma mass spectrometer (ICP-MS). Quality control (QC) samples were run in each batch and included two reagent blanks, two blank spikes, two matrix spikes, and two replicate analyses of field samples. Method detection limits were 5.0 mg/kg dw for Al and Fe, 1.0 mg/kg dw for Zn, 0.5 for Pb, and 0.05 for Cd. Accuracy was assessed on the high end in each batch with Buffalo River sediment (NIST 2704) to take into account the high dust content of Stratum 1 samples. *Hylocomium splendens* reference material (M2; Steinnes et al. 1997) was obtained from the Finnish Forest Research Institute and run in each batch as well. Standard performance on peach leaves (NIST 1547) was assessed in a separate run. Quality assurance (QA) targets were $\pm 20\%$; one batch required blank correction for Cd. A comprehensive moss QA review document is available in stand-alone form from the NPS (Ford 2004a).

Soils

A ca. 200 g aliquot of each dried, homogeneous sample was digested in the same manner as the moss samples, and all elements were analyzed by ICP-MS. QC samples included four reagent blanks, two pairs of matrix spikes, and two replicates analyses of field samples. Method detection limits were 2.0 mg/kg dw for Al and Fe, 1.0 mg/kg dw for Zn, 0.2 mg/kg dw for Pb, and 0.02 mg/kg dw for Cd. Accuracy was assessed using Buffalo River sediment (NIST 2704) and Canadian Research Council reference material sediments BCSS-1 and PACS-2. QA targets were $\pm 20\%$; all batches required blank correction for Al, which was above the method detection limit in reagent blanks but well below concentrations in field samples. A comprehensive soil QA review document is available in stand-alone form from the NPS (Ford 2004b).

Spatial Analysis

Spatial Coordinates

Our analysis uses a geostatistical spatial model based on points and distances, so latitude and longitude were recorded for all sample units. To make *x*- and *y*-coordinates comparable, we considered the Universal Transversal Mercator (UTM) projection. However, the whole study area crosses more than one UTM zone, and because distortion

increases away from the central meridian, we transformed the geographical coordinates according to the Transversal Mercator projection based on a central meridian that was the mean of all of the longitude coordinates of our data.

Explanatory variables

Explanatory variables included distance from haul road, distance from port site, and side of road (i.e., north vs. south). Distance variables were transformed with the natural logarithm (ln).

Spatial Linear Model

To analyze our data ($n = 226$), we used a spatial linear model (e.g., Ver Hoef et al. 2001). The spatial linear model can be written as,

$$\mathbf{y} = \mathbf{X}\boldsymbol{\beta} + \boldsymbol{\varepsilon} \quad (1)$$

where \mathbf{y} is a vector for the response variable (ln of Pb, Zn, or Cd), \mathbf{X} is a design matrix containing the explanatory variables, $\boldsymbol{\beta}$ is a vector of parameters, and $\boldsymbol{\varepsilon}$ is a vector of random errors. In classical linear models, it is often assumed that $\text{var}(\boldsymbol{\varepsilon}) = \sigma^2\mathbf{I}$, that is, all errors are independent. We relaxed this assumption and allowed the errors to be spatially autocorrelated so $\text{var}(\boldsymbol{\varepsilon}) = \boldsymbol{\Sigma}_{\boldsymbol{\theta}}$, where $\boldsymbol{\Sigma}_{\boldsymbol{\theta}}$ is the covariance matrix and we show its dependence on spatial autocorrelation parameters $\boldsymbol{\theta}$. Autocovariance was modeled based on the distances between all pairs of points. We used the exponential autocovariance model,

$$C_{\boldsymbol{\theta}}(h) = \theta_1 I(h = 0) + \theta_2 \exp(-h/\theta_3) \quad (2)$$

where h is the distance between any two points, $I(a)$ is the indicator function (equal to 1 if the expression a is true, otherwise it is 0), and the vector $\boldsymbol{\theta}$ contains three parameters: the nugget θ_1 , partial sill θ_2 , and range θ_3 . The goal of the analysis was to estimate $\boldsymbol{\beta}$ and $\boldsymbol{\theta}$; $\boldsymbol{\beta}$ contains the slope parameters of our regression model, and to estimate $\boldsymbol{\beta}$ and obtain variances of these estimates, we need to know $\boldsymbol{\theta}$. We chose restricted maximum likelihood (REML) to estimate $\boldsymbol{\theta}$. The usual geostatistical methods of estimating variograms are not appropriate here because we are modeling the errors, which are not directly observable. For these cases, maximum likelihood (ML) and REML are better.

However, ML is known to be more biased than REML (Mardia and Marshall 1984; Ver Hoef and Cressie 2001). REML creates a likelihood that depends only on θ by integrating over all possible values of β , and then we only need to maximize this likelihood. Once θ was estimated, hereafter referred to as $\hat{\theta}$, we proceeded with generalized least squares,

$$\hat{\beta} = (\mathbf{X}'\Sigma_{\hat{\theta}}^{-1}\mathbf{X})^{-1}\mathbf{X}'\Sigma_{\hat{\theta}}^{-1}\mathbf{y},$$

to estimate the regression parameters, and their estimated variances are the diagonal elements of

$$\text{var}(\hat{\beta}) = (\mathbf{X}'\Sigma_{\hat{\theta}}^{-1}\mathbf{X})^{-1}.$$

All parameters β and θ were fit using PROC MIXED in SAS. Degrees of freedom used the Satterthwaite option (Satterthwaite 1941), which helps to account for the uncertainty in covariance parameter estimates by adjusting the degrees of freedom. For a modern view, see Kenward and Roger (1997).

Model Selection

Based on a pilot study and exploratory data analysis of bivariate plots, it appeared that the most important factors affecting variation in the response variables were distance from haul road, distance from port site, and side of the road (a categorical variable indicating north or south of haul road). We included these variables in the model, as well as all of their interactions. All three variables were important in most models, as were the (distance from haul road) \times (distance from port) and (side of road) \times (distance from haul road) interactions. Thus, we included all three main effects and these two interactions in all models. Residuals were checked using Q-Q plots (Wilk and Gnanadesikan 1968) and appeared to be normally distributed in all cases. To assess autocorrelation structure, we visually examined empirical semivariograms of the residuals and used AIC to determine whether anisotropy was necessary. Using both methods, there was no evidence of anisotropy in the residuals.

Coefficient of Determination - R^2

In the classical linear model, the random errors of (1) are assumed independent, and one way to write R^2 is

$$R^2 = 1 - \frac{(\mathbf{y} - \mathbf{X}\hat{\boldsymbol{\beta}})'(\mathbf{y} - \mathbf{X}\hat{\boldsymbol{\beta}})}{(\mathbf{y} - \mathbf{1}\hat{\mu})'(\mathbf{y} - \mathbf{1}\hat{\mu})}$$

where $\mathbf{1}$ is a vector of ones, and $\hat{\boldsymbol{\beta}} = (\mathbf{X}'\mathbf{X})^{-1}\mathbf{X}'\mathbf{y}$ and $\hat{\mu} = \bar{y}$. For the situation where the errors have covariance matrix $\boldsymbol{\Sigma}_{\hat{\theta}}$, let $\tilde{\mathbf{y}} \equiv \boldsymbol{\Sigma}_{\hat{\theta}}^{-1/2}\mathbf{y}$, $\tilde{\mathbf{X}} \equiv \boldsymbol{\Sigma}_{\hat{\theta}}^{-1/2}\mathbf{X}$ and $\tilde{\boldsymbol{\varepsilon}} = \boldsymbol{\Sigma}_{\hat{\theta}}^{-1/2}\boldsymbol{\varepsilon}$. Then $\tilde{\mathbf{y}} = \tilde{\mathbf{X}}\boldsymbol{\beta} + \tilde{\boldsymbol{\varepsilon}}$ is model (1) with independent errors, so we took

$$R^2 = 1 - \frac{(\tilde{\mathbf{y}} - \tilde{\mathbf{X}}\tilde{\boldsymbol{\beta}})'(\tilde{\mathbf{y}} - \tilde{\mathbf{X}}\tilde{\boldsymbol{\beta}})}{(\tilde{\mathbf{y}} - \mathbf{1}\tilde{\mu})'(\tilde{\mathbf{y}} - \mathbf{1}\tilde{\mu})} = 1 - \frac{(\mathbf{y} - \mathbf{X}\hat{\boldsymbol{\beta}})'\boldsymbol{\Sigma}_{\hat{\theta}}^{-1}(\mathbf{y} - \mathbf{X}\hat{\boldsymbol{\beta}})}{(\mathbf{y} - \mathbf{1}\hat{\mu})'\boldsymbol{\Sigma}_{\hat{\theta}}^{-1}(\mathbf{y} - \mathbf{1}\hat{\mu})}, \quad (3)$$

where $\tilde{\boldsymbol{\beta}} = (\tilde{\mathbf{X}}'\tilde{\mathbf{X}})^{-1}\tilde{\mathbf{X}}'\tilde{\mathbf{y}}$, $\tilde{\mu} = \bar{\tilde{y}}$, $\hat{\boldsymbol{\beta}} = (\mathbf{X}'\boldsymbol{\Sigma}_{\hat{\theta}}^{-1}\mathbf{X})^{-1}\mathbf{X}'\boldsymbol{\Sigma}_{\hat{\theta}}^{-1}\mathbf{y}$, and $\hat{\mu} = (\mathbf{1}'\boldsymbol{\Sigma}_{\hat{\theta}}^{-1}\mathbf{1})^{-1}\mathbf{1}'\boldsymbol{\Sigma}_{\hat{\theta}}^{-1}\mathbf{y}$.

Spatial Predictions

Among the aims of the analysis was to predict the response variable for points and bands and to estimate the surface area in various concentration categories. Because the data were log-transformed, there are well-known difficulties in making predictions on the log scale and then back-transforming to the original scale (e.g., Cressie 1993, p. 136). This is made more difficult by the fact that we have covariates, measurement error, and we wanted to make estimates of complex functions of the predictions (total area above a reference level). Therefore, we used a Bayesian approach to conditional simulation to estimate all quantities. Our method followed De Oliveira et al. (1997) using a log transformation and the exponential covariance (2), but using the reference prior described by Berger et al. (2001). We had samples for 3 locations measured twice, and we had an independent data set of 13 samples that the lab measured twice. Assuming each sample had a unique mean, we used the 13 samples to develop a standard posterior for a variance parameter for measurement error, e.g., an inverse- χ^2 (Gelman et al. 1995, p. 237). We then used this posterior as a prior on θ_{ME} for a partitioned nugget effect in (2) so that $\theta_1 = \theta_{MS} + \theta_{ME}$, where θ_{ME} is the variance due to measurement error and θ_{MS} is the

variance due to microscale variation (*sensu* Cressie 1993, p. 59). Although measurement error is present in the observed data, we are not interested in predicting values with measurement error, so we filtered it out by letting $\theta_1 = \theta_{MS}$ when forming the posterior predictive distribution.

Predictions were made on a grid. The prediction grid was patterned after the actual sampling grid (described above) where cell size increased with distance from the haul road. The final prediction grid contained 6000 cells. A total of 200 simulations were run (on the prediction grid) for each element. The predictions at each location were back-transformed from the log scale, and then means over the 200 simulations were used to create interpolation maps; quantiles over the 200 simulations provided uncertainty estimates for the interpolations.

The area of heavy metal deposition was estimated by computing the proportion of the prediction grid values above a given reference level for each simulation in each strata and then multiplying each proportion times the area of the stratum. Based on 200 simulations, means and standard deviations were then calculated from these estimates. Confidence intervals were derived using percentiles from the simulations.

Mapping

Interpolation and contour maps were created from the prediction grid means in ArcView 3.2 with Spatial Analyst (ESRI 1996) using the inverse distance weighted technique (IDW) with 12 nearest neighbors and power = 2. IDW was used because it is an exact interpolator and was a quick and efficient technique for dealing with thousands of grid points. Several power values were tested, but little change was noted due to the denseness of the grid. Isolines for interpolation maps and categories for estimating areal extent in the ten moss concentration categories were constructed using a combination of the following objective criteria: (1) quantiles from regional Arctic Alaska moss heavy metal concentration data (Ford et al. 1995) and (2) median heavy metal concentrations from the 'cleanest' stratum (# 7) within the current study area and their multiples (e.g., 10X, 20X, etc.). Subjective intervals based primarily on natural breaks were added

where deemed necessary to provide the best graphical representation of spatial patterns, but these were kept to a minimum.

RESULTS

Summary Data

Summary data for analytes in moss and soil across the entire study area are summarized in Table 3. The moss data show a high degree of variability (2–3 orders of magnitude) for all elements due to the large differences between areas with greater and lesser heavy metal levels. Log transformation greatly improved the normality of distributions. By contrast, heavy metal concentrations in subsurface soils show relatively low variability.

Table 3. Summary data for analytes in moss and subsurface soil throughout the entire study area, including median, mean, standard deviation (SD), and range of values. All units are in mg/kg dw.

Substrate (<i>n</i>)	Element	Median	Mean	SD	Range
Moss (<i>n</i> = 151)	Cd	0.56	1.86	3.54	0.08 – 24.30
	Pb	16.2	68.1	141.1	1.1 – 912.5
	Zn	92	292	518	2 – 3,207
	Al	773	4,850	10,243	46 – 45,749
	Fe	580	3,063	6,242	168 – 28,630
Soil (<i>n</i> = 46)	Cd	0.27	0.27	0.13	0.07 – 0.75
	Pb	15.3	17.8	11.7	7.8 – 83.8
	Zn	96	96	24	49 – 164
	Al	61,350	60,760	11,518	25,900 – 86,600
	Fe	39,750	39,339	12,559	14,400 – 71,800

Elemental Correlations in Moss

Correlation coefficients were calculated among analytes in *H. splendens* moss (Table 4). Two distinct groups were readily apparent: heavy metals ($0.94 > r^2 > 0.92$) and crustal elements ($r^2 = 0.99$). The three heavy metals (Cd, Pb and Zn) are geochemically related and typically co-occur in metal sulfide deposits such as those at the mine site. At Red Dog Mine, Cd is present in Pb and Zn concentrates at levels of approximately 820 ppm (0.08%) and 2980 ppm (0.30%) respectively (Exponent 2002a). The crustal elements (Al and Fe) exhibited a near 1:1 relationship; Al is therefore used to represent crustal elements in the analyses that follow. Somewhat weaker correlations ($0.79 > r^2 > 0.72$) were observed between crustal elements and heavy metals (Table 4).

Table 4. All pairwise correlation coefficients among element concentrations in *Hylocomium splendens* moss ($n = 151$). All data were \log_{10} transformed.

	Cd	Pb	Zn	Al	Fe
Cd	1.00	0.94	0.94	0.79	0.79
Pb	0.94	1.00	0.92	0.72	0.74
Zn	0.94	0.92	1.00	0.77	0.79
Al	0.79	0.72	0.77	1.00	0.99
Fe	0.79	0.74	0.79	0.99	1.00

Spatial Regression

Spatial regression was used to examine relationships between element concentrations in moss and various factors potentially associated with metal deposition (Table 5). Overall fit of the models was excellent for heavy metals with R-squared values ranging from 0.83 – 0.86. The Al model also demonstrated a good fit with an R-squared value of 0.70. Several of the independent variables were found to have significant predictive power,

Table 5. Spatial regression results examining relationships between moss concentrations and potential sources of airborne deposition across the entire study area. All distance variables and element concentrations were log (ln) transformed. Results are based on 232 observations, including random and field duplicates. Degrees of freedom (DF) were calculated using the Satterthwaite option in SAS PROC MIXED.

Effect	Cd Model			Pb Model			Zn Model			Al Model		
	Esti- mate	DF	F P-value	Esti- mate	DF	F P-value	Esti- mate	DF	F P-value	Esti- mate	DF	F P-value
Intercept	13.12	90		15.79	92		14.42	55		11.41	49	
Side of Road – North	0.12	157	0.566	-0.58	50	5.6 0.022	-0.22	136	1.1 0.296	-0.46	123	1.3 0.266
Side of Road – South	0			0			0			0		
Distance to Road	-1.52	100	<0.001	-1.21	144	18.7 <0.001	-0.95	160	18.7 <0.001	-1.05	132	6.0 0.015
Distance to Port	-1.04	88	<0.001	-0.79	97	8.8 0.004	-0.50	72	5.5 0.022	0.13	57	0.1 0.751
Distance to Road x Side of Road – North	0.05	153	0.059	0.19	16	23.0 <0.001	0.12	70	9.8 0.003	0.17	61	5.9 0.018
Distance to Road x Side of Road – South	0			0			0			0		
Distance to Road x Distance to Port	0.11	98	<0.001	0.05	138	4.0 0.048	0.04	156	3.4 0.068	0.03	128	0.6 0.427
R ²	0.86			0.83			0.85			0.70		

including (1) distance to the haul road, (2) distance to the port site, and (3) north versus south side of road. “Distance to the haul road” was significant for all elements ($p < 0.001$ for heavy metals) in spatial regression (Table 5). Figure 3a further illustrates strong road-related gradients encompassing the study area on both sides of the road. These results build upon earlier research (Ford and Hasselbach 2001) by greatly expanding the known extent of heavy metal escapement from the haul road. Aluminum showed a somewhat weaker relationship with distance to haul road ($p = 0.015$) than was evidenced by the heavy metals.

Concentrations of all three heavy metals in mosses demonstrated statistically significant relationships ($p < 0.01$) with distance to the port site (Table 5). This correlation was not found for Al ($p = 0.751$). The variable “side of road” (indicating north or south side of the haul road) had significant predictive power in and of itself for Pb only ($p = 0.02$). However, when entered in spatial regression models as an interaction term with “distance to haul road”, it was highly significant ($p < 0.01$) for Pb and Zn and nearly significant ($p = 0.06$) for Cd.

Patterns of Heavy Metal Deposition

Spatial patterns estimated by interpolated conditional simulation maps were similar for all elements and consisted of concentric bands of decreasing deposition radiating from the haul road and port site (Figures 4 & 5).

Mapped patterns depicting strong haul road and port site gradients are consistent with spatial regression results. High levels of heavy metals along the haul road corridor are readily apparent (Figures 4 & 5). Roadside concentrations (i.e., Stratum 1: 0 – 10 m from haul road) ranged from 7–24 mg/kg dw for Cd and 271–912 mg/kg dw for Pb. Highest values (e.g., Pb legend class: 400–1000 mg/kg dw) occurred along the portion of the haul road nearest to the port site for all analytes (e.g., Figure 6).

Figure 3. Elemental concentrations in moss and subsurface soil with respect to the DMTS haul road. The midline of the road is represented by location “0” on the X-axis. The south side of haul road is displayed as negative values, whereas the north side of the road is shown as positive. Mean soil depth = 62 cm. All data were log₁₀ transformed.

Figure 3a. Moss (*n* = 151)

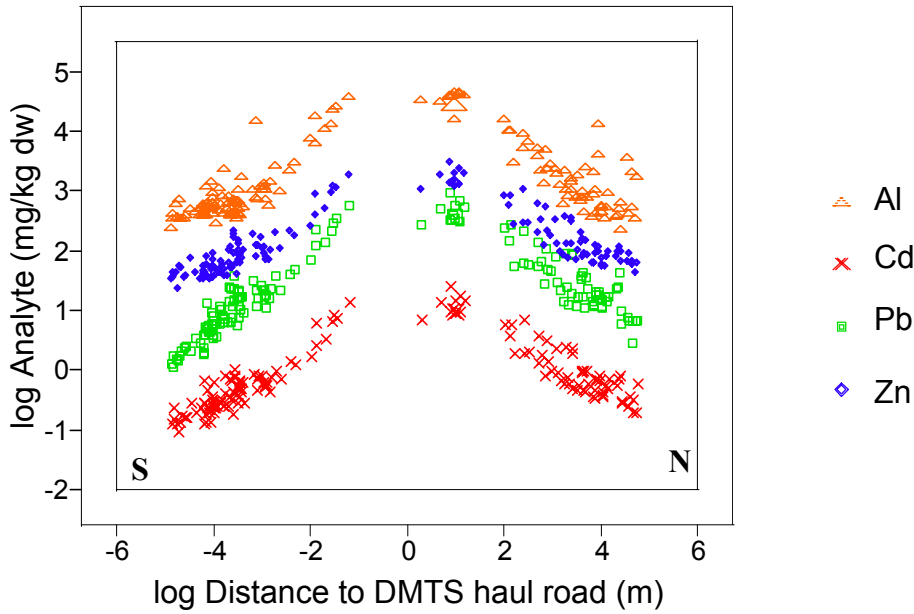


Figure 3b. Subsurface soil (*n* = 46)

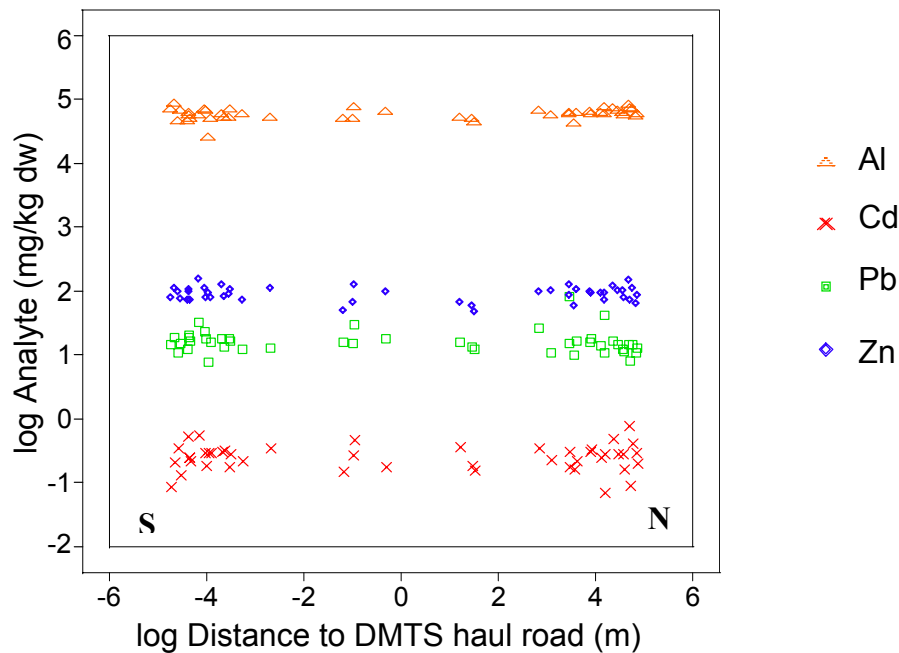
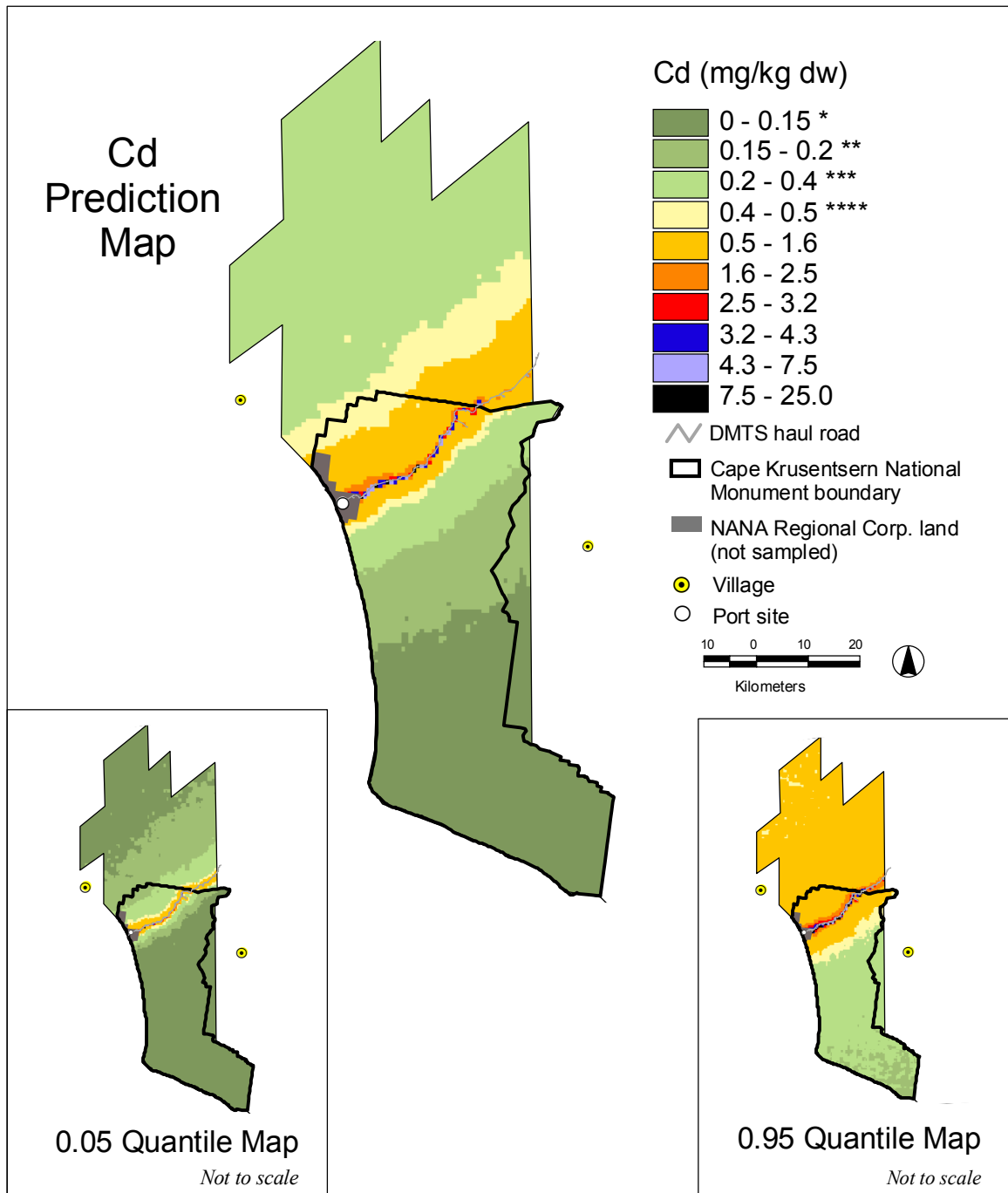
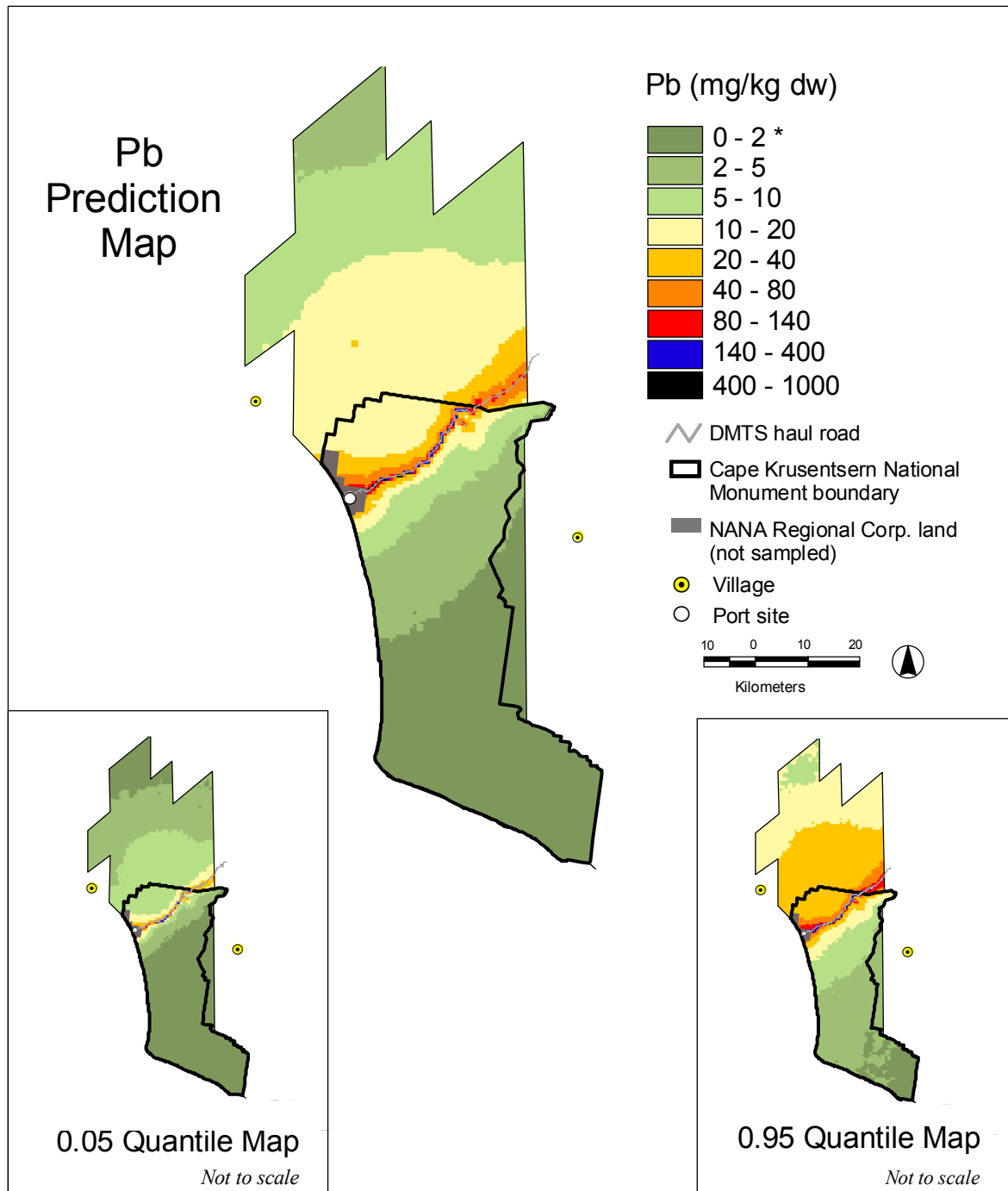


Figure 4. Conditional simulation predictions for moss Cd concentrations in the vicinity of Cape Krusenstern National Monument including 0.05 and 0.95 prediction quantiles.



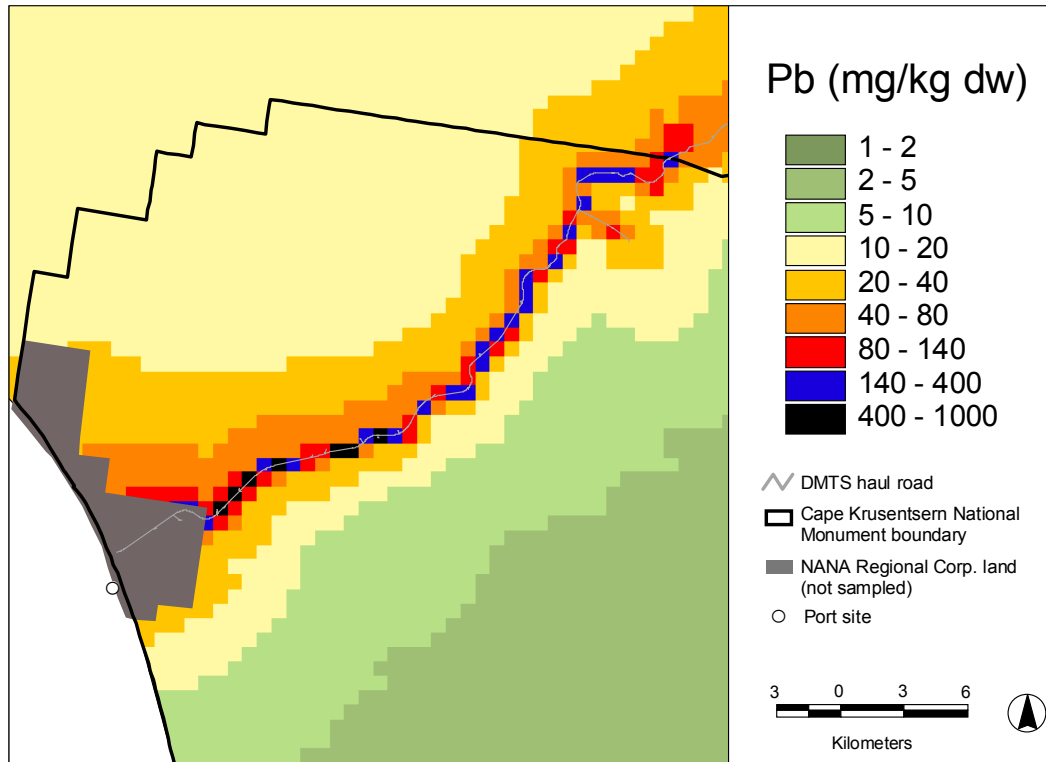
* Ford et al. (1995) Arctic Alaska median = 0.15 mg/kg dw Cd
 ** Ford et al. (1995) Arctic Alaska 75th percentile = 0.23 mg/kg dw Cd
 *** Ford et al. (1995) Arctic Alaska 90th percentile = 0.41 mg/kg dw Cd
 **** Ford et al. (1995) Arctic Alaska maximum = 0.48 mg/kg dw Cd

Figure 5. Conditional simulation predictions for moss Pb concentrations in the vicinity of Cape Krusenstern National Monument including 0.05 and 0.95 prediction quantiles.



* Ford et al. (1995) Arctic Alaska maximum = 2.3 mg/kg dw Pb

Figure 6. Conditional simulation predictions for moss Pb concentrations along the DMTS haul road corridor.

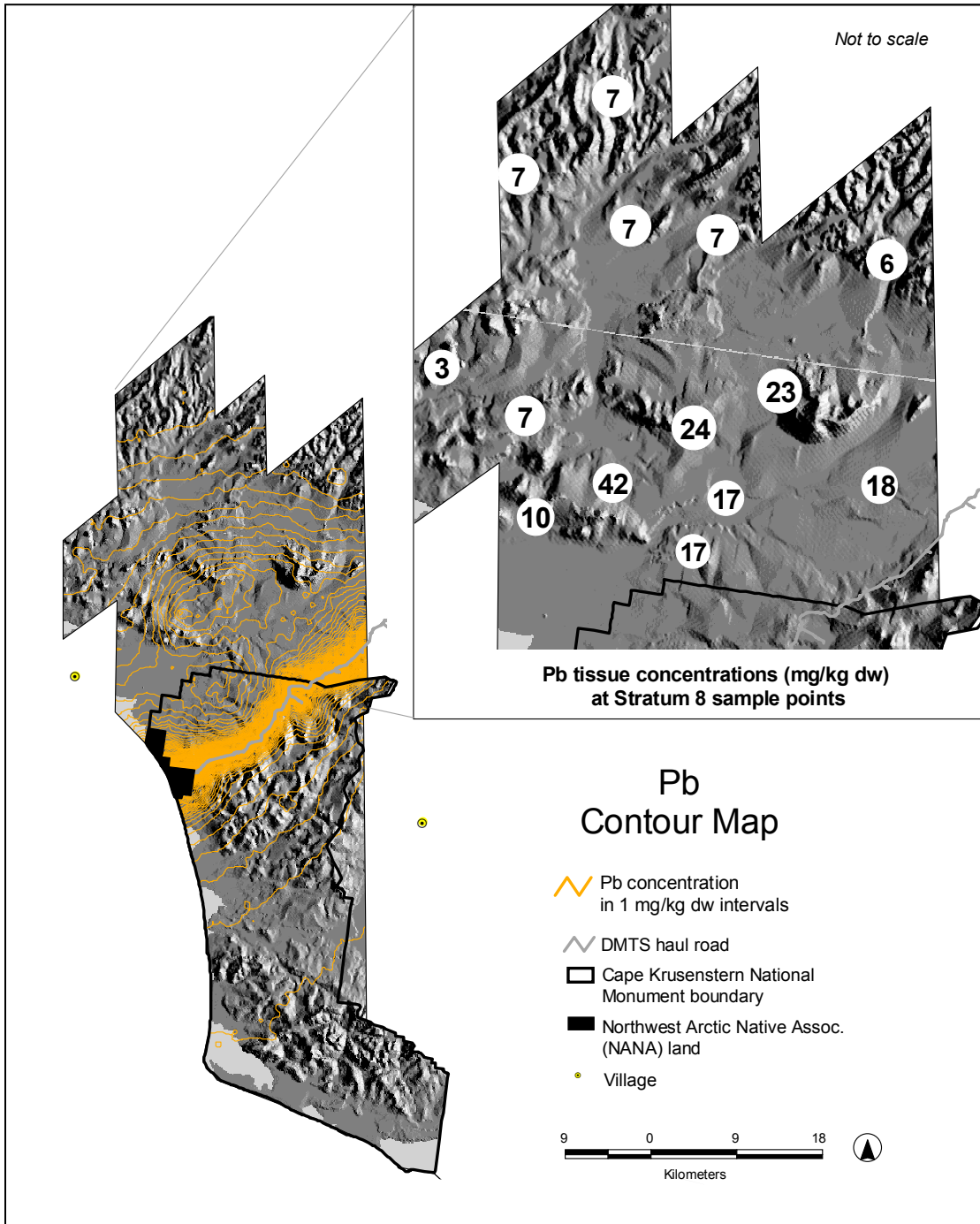


The port gradient itself is displayed as a band of heavy metal deposition around the facility. The pattern is most pronounced to the north-northeast of the facility (Figure 6). Sampling was conducted along the NPS-NANA port boundary located 3–4 km from the actual port site (Figure 2). Heavy metal levels in mosses in this area ranged from 20–140 mg/kg Pb and 0.7–3.6 mg/kg Cd.

Mapped patterns also reveal the differences between heavy metal levels north and south of the haul road detected by spatial regression results (Figures 4 & 5). In general, heavy metal concentrations in moss decrease more gradually with distance on the north side of the haul road than on the south. In the far southern portion of the Monument, metal levels continue to decrease consistently, reaching their lowest levels (median Cd = 0.16 mg/kg dw; median Pb = 2.0 mg/kg dw) in the vicinity of the Igichuk Hills, 40 km from the haul road. This contrasts with the northern portion of the study area where concentrations remain relatively high (20–40 mg/kg dw Pb) 4–40 km north of the haul road and Pb levels at the most distant points (60 km north of the haul road) are 3–4 times those in the Igichuk Hills in the far southern portion of the study area.

To further investigate depositional patterns north of the haul road, Pb levels in moss are displayed using both interpolated contour intervals and raw data values derived from conditional simulation modeling (Figure 7). Results indicate that Pb levels in Kisimilot/Iyikrok hills, 25 km north of the haul road, range from 7 to 42 mg/kg dw (Figures 1 & 7-inset). North of this area, Pb concentrations decrease to somewhat lower values (ca. 7 mg/kg dw).

Figure 7. Moss Pb concentration contours (derived from conditional simulation) overlain on topography in the vicinity of Cape Krusenstern National Monument. Inlay shows actual Pb concentrations in the northern portion of the study area. Moss concentrations were rounded for ease of viewing.



Subsurface Soils

Subsurface soils were analyzed to ascertain whether subsurface geochemistry at the sample points was the underlying cause of the differences observed in moss elemental levels within the study area. Figure 3b shows that elemental concentrations in subsurface soils are uniform throughout the study area regardless of side of road or distance from haul road. This contrasts with the moss overlay plot in Figure 3a showing a strong haul road-related gradient. Therefore, higher levels of heavy metals in mosses observed in portions of the study area do not appear to be associated with differences in subsurface geochemistry at the sample points.

Regional Context

No site-specific baseline data exist with which to estimate natural, pre-mine surface conditions in and around the Monument. Wiersma et al. (1986) studied heavy metal concentrations in *H. splendens* moss on and near a gravel bar with a long history of motorized air and watercraft use in Noatak National Park. Methods appear to be similar to those used here, although the digestion method is not given. Instead of using just the most recent 3–5 segments, however, these authors used the whole plant, which gives concentrations ca. 2x those obtained using just the 3–5 distal segments (Ford, unpublished data), probably reflecting accumulation of heavy metals over a longer time frame. Further, there is no indication that moss samples were cleaned of visually obvious debris. The authors of the study considered their Pb results to be undesirably variable (coefficient of within-site variation ca 1.2), and Cd analyses failed accuracy QC checks. For all of these reasons, as well as the fact that the sampling location likely included Pb deposition from local motorized traffic over several years, the Wiersma et al. (1986) data on Pb and Cd are considered unsuitable for comparison with the present study.

A series of *H. splendens* studies was also done by Crock and colleagues for lower latitude regions of Alaska (Crock et al. 1992a, 1992b, 1993). The Denali study is the most pertinent to the current work, although it included intensive sampling near a 25-horsepower coal-fired power plant. Crock et al. (1992a) note that observed Pb levels may be associated with this source. Further, the method detection limit for Cd was relatively

high, and most of their Cd data fell below that value. As in the Wiersma et al. (1986) study, whole moss was used instead of clipping to include just the past 3–5 years. Unlike the present study, mosses in the Crock et al. studies were washed, presumably because dry deposition was not of interest. For all these reasons, the Crock et al. studies are also considered unsuitable for comparison with the present study.

Ford et al. (1995) conducted a regional study of heavy metal concentrations in *H. splendens* moss in Arctic Alaska. That study included three sites located 35–120 km east-northeast of the Red Dog mine site, as well as 10 sites in western Arctic Alaska sampled as part of a pilot grid-based objective sampling campaign. The laboratory and field methods were virtually identical to those used in this study. Therefore, we compare our data for northwestern Alaska to the data in that regional study.

Relative to these regional data, the areas surrounding the haul road and port site contain highly elevated levels of heavy metals (Tables 6 & 7; Figures 4 & 5). South of these areas, Cd levels drop below the maximum concentrations reported by Ford et al. (1995) just north of the crest of the Tahinichok Mountains, 3 km from the haul road (Figures 1 & 4). In contrast, Pb levels do not drop below even the 90th percentile of concentrations reported by Ford et al. (1995) until 40 km south in the vicinity of the Igichuk Hills (Table 7; Figures 1 & 5).

To the north, moss Cd levels are between the 75th percentile and the maximum concentrations reported by Ford et al. (1995) (Table 6, Figure 4). This is in contrast to Pb levels that exceed maximum concentrations reported by Ford et al. (1995) throughout the northern portion of the study area (Table 7; Figure 5).

Table 6. Comparison of Cd concentrations in *Hylocomium splendens* moss in the current study area with Arctic Alaska values reported by Ford et al. (1995). Moss concentration is given as mg/kg dw.

	Cd median	Cd 75 th percentile	Cd 90 th percentile	Cd range
<i>Current study:</i>				
< 10 m from DMTS haul road (Stratum 1)	11.60	14.00	21.93	6.87 – 24.31
> 10 m from DMTS haul road (Strata 2 – 8)	0.536	0.80	2.23	0.09 – 7.98
<i>Regional data:</i>				
Ford et al. 1995	0.15	0.23	0.41	0.02 – 0.48*

* One data point (Cd = 0.98 mg/kg dw) was omitted based on problems described by the primary author regarding possible sample contamination during sample transport (J. Ford, pers. comm.).

Table 7. Comparison of Pb concentrations in *Hylocomium splendens* moss in the current study area with Arctic Alaska values reported by Ford et al. (1995). Moss concentration is given as mg/kg dw.

	Pb median	Pb 75 th percentile	Pb 90 th percentile	Pb range
<i>Current study:</i>				
< 10 m from DMTS haul road (Stratum 1)	448.0	842.2	842.2	271.1 – 912.5
> 10 m from DMTS haul road (Strata 2 – 8)	15.1	29.4	91.0	1.1 – 350.3
<i>Regional data:</i>				
Ford et al. 1995	0.6	0.8	1.4	0.4 – 2.3

Geographic Extent of Deposition

Conditional simulation estimates were made of the total area for which moss levels fell into various concentration categories (Table 8). In an estimated 90,210 ha, Cd levels exceeded the maximum concentration for Arctic Alaska reported by Ford et al. (1995)(Tables 6 & 8). In addition, Cd levels in an estimated 453 ha were greater than 5.0 mg/kg dw Cd, or approximately 10 times the maximum concentration reported by Ford et al. (1995)(Tables 6 & 8). For Pb, an estimated 58,067 ha exceeded 20 mg/kg dw, or approximately 10 times the maximum concentration for Arctic Alaska reported by Ford et al. (1995) (Tables 7 & 8). In addition, in approximately 102 ha, Pb levels exceeded 400 mg/kg dw (Table 8). Mosses with the highest heavy metal concentrations were located along the haul road easement within Cape Krusenstern National Monument (Figures 4, 5 & 6).

DISCUSSION

Sources of Heavy Metal Escapement

Strong depositional gradients exist within our study area with regard to the haul road and port site. Earlier work identified the haul road as an important source of heavy metal escapement (Exponent 2002a, Ford and Hasselbach 2001). However, materials used in construction of the haul road did not contain high levels of heavy metals (Exponent 2002a, Ford and Hasselbach 2001), and therefore roadbed materials per se were not believed to be a source of heavy metals. Rather, the main mechanism of haul road escapement appeared to be related to the ore trucks (Exponent 2002a, Ford and Hasselbach 2001). Ore dust generated in the unloading (and loading) process at the port (and mine) site result in contamination of ore truck surfaces. This fugitive dust is then blown by wind (or washed by rain, etc.) from truck surfaces during transit. Figure 6 shows heavy metal levels *along the haul road* decreasing with distance from the port site (see also Exponent 2002a). A similar escapement mechanism may exist at the mine site (Exponent 2002a), although our sample points were too distant from the mine (30–100+ km) to detect such a pattern.

Table 8. Conditional simulation estimates of heavy metal depositional areas within the study area and within Cape Krusenstern National Monument (NPS lands). Values are presented as overall area estimates in hectares (ha). Confidence intervals (CI) are also given.

Element		Entire Study Area		NPS Lands Only*	
	mg/kg dw	area (ha)	CI 5 – 95% (ha)	area (ha)	CI 5 – 95% (ha)
Cd	> 0.5**	90,210	65,829 – 119,935	36,594	32,574 – 41,778
	> 2.0	3,592	2,129 – 5,337	2,937	2,129 – 3,916
	> 5.0	453	306 – 627	450	306 – 627
	> 8.0	159	95 – 234	159	95 – 234
Pb	> 2 ***	447,374	418,653 – 474,240	175,421	150,958 – 198,890
	> 20	58,067	39,910 – 85,505	20,538	17,172 – 24,112
	> 50	10,975	4,839 – 11,860	4,430	3,418 – 5,892
	> 100	2,794	1,032 – 3,912	1,368	1,032 – 1,923
	> 200	397	262 – 760	360	262 – 476
	> 400	102	66 – 146	102	66 – 146

* Including road easement

** Maximum value recorded for Arctic Alaska by Ford et al. (1995) = 0.48 mg/kg dw
Cd

***Maximum value recorded for Arctic Alaska by Ford et al. (1995) = 2.3 mg/kg dw Pb

Up to 1.3 million wet metric tons of Pb and Zn concentrate (roughly equivalent to 9 months of mine output) are stored at the port site and subsequently conveyed to barges during the ice-free shipping season (Glavinovich pers. comm. 2004, Exponent 2002b). Surface soil Pb levels in excess of 27,000 mg/kg (27x the U.S. Environmental Protection Agency's industrial soil cleanup standard of 1000 mg/kg) were reported near port facility operational areas in a 1996 monitoring summary (Exponent 2002c, Exponent 2001). It is not surprising, then, that our regression results showed significant relationships between distance to the port site and concentrations of all three heavy metals in mosses (Table 5).

The strong relationship between Cd and distance to the port site merits attention as additional factors may be involved (Table 5). Part of the relationship may be attributable to a maritime effect resulting in higher Cd in the immediate vicinity of coastlines. For example, analysis of snow samples collected from the Chukchi Sea, the Beaufort Sea, and inland environments has suggested a maritime effect for Cd (Garbarino et al. 2002). In the current study, the relationship between Cd and distance to the port site may not be fully separable from the relationship with distance to the sea. Further, Ford et al. (1995) found variable Cd concentrations in inland Arctic Alaskan samples of *H. splendens* moss that were not explained by either slope position or associated vegetation type. These authors suggested that a combination of factors "combining lithological sources with landscape setting and hydrological factors" play a role in determining moss Cd concentrations in pristine environments. Though both distance to port site and distance to the haul road are certainly major explanatory variables for gross spatial patterns of Cd concentrations, more work is required to understand finer scale variation of Cd in the study area and the region.

Heavy Metals and Dust

There are both similarities and differences between the distribution of heavy metals (Cd, Pb, and Zn) and the crustal elements present in dust (Al, Fe). Both show significant relationships with distance to the haul road, although the relationship is weaker for Al than for heavy metals ($p = 0.015$ vs. $p < 0.001$)(Table 5). The relationships with the port site are quite different, however; Al demonstrated a distinct lack of relationship to

distance to the port site (Table 5). This is probably due to the fact that traffic slows considerably in the vicinity of the port site, thereby mobilizing less dust and weakening the “dust signal” from that area.

Although strong correlations were observed between the heavy metal group and crustal element group, within-group correlations were found to be somewhat stronger than between-group correlations (Table 4). This is likely because sources of the two groups of elements, although related in many ways, also include independent contributions. For example, as discussed above, heavy metal escapement along the haul road corridor has been attributed to windblown dispersal of concentrate from ore truck surfaces. Vehicles other than ore trucks would be expected to mobilize primarily road dust. In addition, naturally occurring dust (e.g., deflation from river deposits and cryogenically exposed soils) is likely to contribute additional Al and Fe to moss surfaces over time. Both of these processes infuse additional crustal elements into the environment that would effectively weaken the correlation between heavy metals and crustal elements. The relationship is likely to be further complicated by several factors. For example, generation of road dust may be minimal when the roadbed is frozen and/or snowcovered, but escapement from ore truck surfaces is presumably continuous throughout the year. Particle size and weight may also be important. The particle size of naturally occurring crustal elements is likely to be larger than the finely ground heavy metal concentrate, and therefore would not be expected to disperse as far. On the other hand, Al and Fe in the roadbed are probably crushed by the weight of passing vehicles into finer and lighter materials that may travel farther than might otherwise be expected. Regardless of these differences, the strength of the between-group correlations suggests that important depositional pathways are shared by road dust and ore concentrate.

Topography and Wind as Related to Moss Concentrations

One of the prominent features depicted in conditional simulation maps (and confirmed by spatial regression analyses) is the difference between moss concentration patterns on the north and south side of the haul road (Figures 3, 4 & 5 and Table 5). The physical barriers and transport pathways formed by various topographic features are consistent

with these and other patterns. Seasonal winds from the west and south (Exponent 2002a) are probably a contributing factor driving deposition north of the haul road. Local topography also appears to influence patterns of heavy metal deposition, constraining deposition to a narrower swath on the south vs. north side of the road. For example, immediately south of the haul road, airborne deposition is constrained by the Tahinichock Mountains (elevation 502 m, Figure 1). Elevated heavy metal levels encroach on the mid and upper slopes of the north-facing mountain slopes but decrease steadily over the crest to the south (Figure 7). The result is the compressed depositional pattern observed 0–5 km south of the haul road corridor. Conversely, depositional intervals north of the haul road are noticeably broad (Figures 4, 5 & 7). Lead deposition in the 10–20 mg/kg dw range is especially pronounced 4–30 km north of the haul road where the gently sloping terrain drains toward the Omikviorok River, providing little topographic impediment to airborne contaminant movement (Figure 7).

The interaction of wind and topography may also cause depositional fallout in certain areas. The Kisimilot/Iyikrok hills (north of the Wulik River, Figure 1) are a possible example. Moss Pb concentrations are noticeably higher here than in the areas further north (Figure 7-inset). This may reflect deposition of heavy metal-laden dust (mine-related and/or naturally derived) from a focusing effect such as pocket turbulence or the abruptly decreasing wind velocity due to contact with the intermittent topographic features formed by the Kisimilot/Iyikrok hills.

Extent of Depositional Area

In the absence of pre-mine baseline data, it is difficult to directly determine the actual extent of airborne deposition of heavy metals due to ore concentrate escapement in and around the Monument. Earlier work that covered a 1.6 km swath on either side of the haul road (Ford and Hasselbach 2001) noted that moss concentrations of Cd, Pb, and Zn were still elevated at transect points furthest from the haul road relative to maximum concentrations previously reported from undisturbed sites in Arctic Alaska by Ford et al. (1995). In that study, application of enrichment factors (element to Al ratios in mosses vs. local soil parent material) that control for local geology also suggested that concentrate

was still being deposited 1.6 km from the haul road. One of the purposes of the present research was to expand the spatial extent of the earlier studies to gain a clearer picture of the potential depositional area of ore concentrate.

One indication that the full areal extent of heavy metal deposition has been identified would be an obvious 'leveling-off' of moss concentrations at some distance from the haul road. This does not generally occur for Cd and Pb within the study area (Figure 3a).

In the southern portion of the study area, moss concentrations of Cd are less than maximum values previously reported from Arctic Alaska by Ford et al. (1995)(Figure 4; Table 6). In addition, moss Cd concentrations north of the haul road drop below maximum regional values reported by Ford et al. (1995) at a distance of approximately 12 km (Figure 4; Table 6). Collectively, these findings suggest that moss Cd concentrations are unaffected or only slightly affected by mining-related deposition beyond 3 km to the south and 12 km to the north of the haul road. In contrast, Pb levels in the northernmost part of the study area exceed both previously reported Arctic Alaskan maxima (Ford et al. 1995) and concentrations throughout the southernmost parts of the study area (Figure 5; Table 7). In the Kisimilot/Iyikrok hills (north of the Wulik River, Figure 1), moss Pb concentrations ranged from 7 to 42 mg/kg dw ($n = 5$), exceeding the maximum Pb value of 2.3 mg/kg dw reported by Ford et al. (1995). This fact, combined with the strength of the road-related Pb gradient revealed by our analyses (Figures 3 & 5 and Table 5), suggests that mining-related Pb deposition extends at least as far north as the Kisimilot/Iyikrok hills, 25 km from the haul road.

Interpretation of Pb patterns in this northernmost portion of the study is complicated by the geochemical makeup of the broader region. This seems especially true for the area north of the Kisimilot/Iyikrok hills where Pb levels decrease to approximately 7 mg/kg dw (Figure 7-inset). Our results suggest that subsurface geochemistry at sampling points is not responsible for elevated moss concentrations of heavy metals (Figure 3b). However, areas of natural Pb/Zn mineralization are known to exist northwest and northeast of the mine site (Kelley and Hudson 2003, Exponent 2002b).

Due to the lack of a vascular system, mosses do not actively take up elements from substrate. Therefore, Pb levels reflect atmospheric deposition. Thus, higher Pb levels from mosses in the far northern portion of the study area may be attributable to (1) airborne deposition from mining-related activities (e.g., fugitive dust), (2) airborne deposition from weathering of naturally enriched Pb/Zn surface deposits in the broader region, or (3) a combination of the two. Sampling intensity in the northernmost portion of the study area was relatively low, and as a result, the prediction standard error for this area was high (Figures 5 & 7). Additional sampling, both within the far northern portion of the current study area and beyond the study area boundary to the north, is needed to better understand patterns and sources of heavy metal concentrations in this area.

Finally, our study was centered on National Park Service lands 50 km west of the actual mine site and was not designed to examine spatial patterns of heavy metal deposition in the vicinity of the mine itself which could be an important contributor to observed spatial patterns of heavy metal concentrations in *H. splendens* moss. Such research is necessary to clarify the patterns and sources of airborne heavy metal deposition in the region.

CONCLUSIONS

Airborne deposition of heavy metals from mining-related activities appears to occur throughout the northern half of Cape Krusenstern National Monument on both sides of the haul road. The depositional area appears to extend north of Monument boundaries to the Kisimilot/Iyikrok hills (north of the Wulik River) and possibly beyond, although more study is needed in this area. Heavy metal concentrations in *Hylocomium splendens* moss were correlated most strongly with (1) distance from the DMTS haul road and (2) escapement from the port site and were not related to subsurface geochemistry. Spatial patterns with respect to the mine site were not studied.

Highest concentrations of heavy metals in mosses were found within 10 m of the haul road. Concentrations in samples at 1–10 m from the haul road ranged from 6.9–24.3

mg/kg dw for Cd and 271–912 mg/kg dw for Pb. In addition, heavy metal concentrations around the port site boundary were relatively high, particularly to the immediate northeast of the facility. Heavy metal levels in this area appear to be linked to the port site itself where soil Pb levels in excess of 27,000 mg/kg were reported near port facility operational areas in 1996.

Heavy metal concentrations in moss decrease rapidly away from both the haul road and the port site. In general, heavy metal concentrations decrease more slowly on the north side of the haul road than on the south. This difference is probably driven by topography and wind patterns. Deposition south of the haul road appears to be constrained by the Tahinichok Mountains which likely function as a wind-shadow thereby protecting the south side of the mountains from deposition related to the haul road. Heavy metal levels continue to diminish southward, reaching a low point near the Igichuk Hills, 40 km from the haul road, where both Cd and Pb concentrations in moss are within ranges previously reported from other parts of Arctic Alaska.

Concentrations of Cd and Pb in moss in the northernmost part of the study area are greater than those in the southernmost part. This difference does not appear to be attributable to local variations in subsurface geochemistry at the sample points. Cd levels appear to be unaffected or only slightly affected by mining-related deposition at distances greater than 12 km north and 3 km south of the haul road. By contrast, Pb levels in moss remain elevated throughout the northern portion of the study area relative to values previously reported from Arctic Alaska. It appears as though mine-related Pb has been deposited in the vicinity of the Kisimilot/Iyikrok hills (north of the Wulik River), 25 km north of the haul road. Potential mechanisms contributing to this phenomenon include localized turbulence and topography, although inputs from natural sources in the broader region cannot be discounted.

For reasons that remain unclear, Pb concentrations in moss north of the Kisimilot/Iyikrok hills remain somewhat elevated (ca. 7 mg/kg dw) relative to moss concentrations in other parts of Arctic Alaska. Higher Pb levels from mosses in the far northern portion of the

study area may be attributable to (1) airborne deposition from mining-related activities (e.g., fugitive dust), (2) airborne deposition from weathering of naturally-enriched Pb/Zn surface deposits in the broader region, or (3) a combination of the two.

Distinguishing between these sources is important to gain a fuller understanding of the role of mining activities in landscape-scale dissemination of heavy metals. Finer scale sampling is needed to better understand potential patterns of heavy metal deposition north of the Wulik River. Additional study with regard to spatial relationships between moss concentrations and the mine site itself is also recommended.

ACKNOWLEDGEMENTS

This research was funded by the National Park Service and by Federal Aid in Wildlife Restoration to the Alaska Department of Fish and Game. We thank the following people for assistance with logistics, study design, field work, analysis and/or editing: Deborah Coffey, Joel Cusick, Doug and Jennifer Houston, Emily Jacklitch, John Martinisko, Bruce McCune, Trent McDonald, Pat Muir, Walter Neitlich, Karen Oakley, Jerry Post, Teck Cominco Alaska Incorporated, Robert Winfree, and Suzy Will-Wolf. Ikayuqtit team members provided useful reviews of this manuscript. Thanks also to anonymous reviewers. Special thanks to Lois Dalle-Molle, Tom Heinlein, Julie Hopkins, and the late Dave Spirtes for support in all phases of this research.

REFERENCES

Aberg G, Steinnes E, and Hjelmseth H. 2001. Source regions and atmospheric deposition of long-range transported Pb in Norway 1977 – 2000 using moss as indicator.

International Symposium on Applied Isotope Geochemistry, 4, Pacific Grove, California, USA. 2001-06-25—06-29.

Berg T and Steinnes E. 1997. Use of mosses (*Hylocomium splendens* and *Pleurozium schreberi*) as biomonitors of heavy metal deposition: From relative to absolute deposition values. *Environmental Pollution* 98 (1): 61-71.

Berg, T, Hjellbrekke A, Rühling Å, Steinnes E, Kubin E, Larsen MM and Piispanen J. 2003. Absolution deposition maps of heavy metals for the Nordic countries based on moss surveys. *Temnord* 2003:505. Nordic Council of Ministers. Copenhagen, DK. 34 pps.

Berger JO, De Oliveira V, and Sansó B. 2001. Objective Bayesian analysis of spatially correlated data. *Journal of the American Statistical Association* 96: 1361-1374.

Cressie N. 1993. *Statistics for Spatial Data*. John Wiley and Sons, New York. 900 pps.

Crock JG, Gough LP, Mangis, DR, Curry KL, Fey DL, Hageman PL and Welsch EP. 1992a. Element concentrations and trends for moss, lichen, and surface soils in and near Denali national Park and Preserve, Alaska. U.S. Geological Survey Open-file Report 92-323. 148 pps.

Crock JG, Severson RC, and Gough LP. 1992b Determining baselines and variability of elements in plants and soils near the Kenai National Wildlife Refuge, Alaska. *Water Air Soil Pollution* 63:253-271.

Crock JG, Beck KA, Fey DL, Hageman PL, Papp, CS, and Peacock TR. 1993. Element concentrations and baselines for moss, lichen, spruce, and surface soils, in and near Wrangell-Saint Elias National Park and Preserve, Alaska. U.S. Geological Survey Open-File Report 93-14. 98 pps.

De Oliveira V, Kedeem B, and Short DA. 1997. Bayesian prediction of transformed Gaussian random fields. *Journal of the American Statistical Association* 92: 1422-1433.

ESRI 1996. ArcView Spatial Analyst. Environmental Systems Research Institute. Redlands, CA.

Exponent 2001. History and Environmental Impacts of DeLong Mountain Transportation System Port Site, Red Dog Operations, Alaska. Unpublished report. Document no. 8601997.001 0301 0801 SS30. Available from Exponent, 15375 30th Place, Suite 250, Bellevue, WA 98007.

Exponent 2002a. Draft 2001 Fugitive Dust Report. DeLong Mountain Regional Transportation System, Alaska. Unpublished report. Prepared for Teck Cominco Alaska Inc. Document No. 8601997.001 0501 0102 SS25. Available from Exponent, 15375 30th Place, Suite 250, Bellevue, WA 98007.

Exponent 2002b. Draft Fugitive Dust Background Document, DeLong Mountain Regional Transportation System, Alaska. Unpublished report. Prepared by Teck Cominco Alaska Inc. and Exponent. Document No. 8601997.001.03020502SS20. Available from Exponent, 15375 30th Place, Suite 250, Bellevue, WA 98007.

Exponent 2002c. Port Site Characterization Sampling and Analysis Plan, DeLong Mountain Regional Transportation System, Alaska. Unpublished report. Prepared for Teck Cominco Alaska Inc. Document No. 8601997.001 1200 0702 SS07. Available from Exponent, 15375 30th Place, Suite 250, Bellevue, WA 98007.

Ford J. 2004a. Quality Assurance Review. Chemical analyses of summer 2001 moss samples by Battelle Marine Sciences Lab. Available from Western Arctic National Parklands, PO Box 1029, Kotzebue, AK 99752, USA.

Ford J. 2004a. Quality Assurance Review. Chemical analyses of summer 2001 soil samples by Battelle Marine Sciences Lab. Available from Western Arctic National Parklands, PO Box 1029, Kotzebue, AK 99752

Ford J. and Hasselbach L. 2001. Heavy metals in mosses and soils on six transects along the Red Dog Mine Haul Road, Alaska. NPS/AR/NRTR-2001/38. Available from Western Arctic National Parklands, PO Box 1029, Kotzebue, AK 99752

Ford J, Landers D, Kugler D, Lasorsa B, Allen-Gil S, Crecelius E, and Martinson J. 1995. Inorganic contaminants in Arctic Alaskan ecosystems: long-range atmospheric transport or local point sources? *Science of the Total Environment* 160/161: 323-335.

Garbarino JR, Snyder-Conn E, Leiker TJ, and Hoffman GL. 2002. Contaminants in arctic snow collected over northwest Alaskan sea ice. *Water, Air and Soil Pollution* 139: 183-214.

Gelman A, Carlin JB, Stern HS, and Rubin DB. 1995. *Bayesian Data Analysis*. Chapman and Hall, London. 526 pps.

Kelley K and Hudson T. 2003. The natural dispersal of metals to the environment in the Wulik River-Ikalukrok Creek area, Western Brooks Range, Alaska. U.S. Geologic Survey Fat Sheet 107-03.

Kenward MG and Roger JH. 1997. Small sample inference for fixed effects from restricted maximum likelihood. *Biometrics* 53: 983-997.

- Mardia KV and Marshall RJ. 1984. Maximum likelihood estimation of models for residual covariance in spatial regression. *Biometrika* 71: 135-146.
- Public Law 96-487. 1980. Alaska National Interest Lands Conservation Act – December 2, 1980, Stat. 2371.
- Public Law 99-96. 1985. A Bill to Amend the Alaska Native Claims Settlement Act, (99th Congress) - September 25, 1985, Section 34.
- Økland T, Økland RH and Steinnes E. 1999. Element concentrations in the boreal forest moss *Hylocomium splendens*: variation related to gradients in vegetation and local environmental factors. *Plant and Soil*, 209:71–83.
- Ross HB. 1990. On the use of mosses *Hylocomium splendens* and *Pleurozium schreberi* for estimating atmospheric trace metal deposition. *Water, Air and Soil Pollution* 50: 63-76.
- Rühling Å and Steinnes E. 1998. Atmospheric heavy metal deposition in Europe 1995-1996. *NORD 98:15*. Nordic Council of Ministers, Copenhagen.
- Rühling Å and Tyler G. 1970. Sorption and retention of heavy metals in the woodland moss *Hylocomium splendens* (Hedw.) Br. et Sch. *Oikos* 21: 92-97.
- Satterthwaite FF. 1941. Synthesis of variance. *Psychometrika* 6: 309-316.
- Shaole W, Zhao Y, Feng X, and Wittmeier A. 1996. Application of Inductively Coupled Plasma Mass Spectrometry for Total Metal Determination in Silicon-containing Solid Samples Using the Microwave-assisted Nitric Acid-Hydrofluoric Acid- Hydrogen Peroxide-Boric Acid Digestion System. *Journal of Analytical Atomic Spectrometry*. 11(4): 287-296.

Steinnes E, Rambæk JP and Hanssen JE. 1992. Large scale multi-element survey of atmospheric deposition using naturally growing moss as biomonitor. *Chemosphere* 25:735-752.

Steinnes E. 1995. A critical evaluation of the use of naturally growing moss to monitor the deposition of atmospheric metals. *Science of the Total Environment* 160/161:243-249.

Steinnes E, Rühling Å, Lippo H, and Mäkinen A. 1997. Reference materials for large scale metal deposition surveys. *Accred. Qual. Assur.* 2:243-249.

Ver Hoef JM and Cressie N. 2001. Spatial statistics: Analysis of field experiments. In Scheiner, S.M. and Gurevitch, J. (eds.), *Design and Analysis of Ecological Experiments*. Second Edition, Oxford University Press, p. 289-307.

Ver Hoef JM, Cressie N, Fisher RN, and Case TJ. 2001. Uncertainty and spatial linear models for ecological data. Pages 214 – 237 in Hunsaker, C.T., Goodchild, M.F., Friedl, M.A., and Case, T.J. (eds.), *Spatial Uncertainty for Ecology: Implications for Remote Sensing and GIS Applications*. Springer-Verlag, New York.

Viereck LA, Dyrness CT, Batten A R, and Wenzlick KJ. 1992. The Alaska vegetation classification. USDA Forest Service Pacific Northwest Research Station, Portland, OR. General Technical Report #PNW-GTR-286.

Wiersma GB, Slaughter C, Hilgert J, McKee A, and Halpern C. 1986. Reconnaissance of Noatak National Preserve and Biosphere Reserve as a potential site for inclusion in the integrated global background monitoring network. U.S. Man and the Biosphere Program, National Technical Information Service, Washington D.C. 84 pps.

Wilk MB and Gnanadesikan R. 1968. Probability plotting methods for the analysis of data. *Biometrika* 55: 1-17.

APPENDIX I

MOSS DATA

Moss Code	Plot Type	Sample Point	Sample No.	Moss Cd (mg/kg dw)	Moss Pb (mg/kg dw)	Moss Zn (mg/kg dw)	Moss Al (mg/kg dw)	Moss Fe (mg/kg dw)
001P-M-01	Primary Pt.	1	1P	10.25	383.19	1528.4	39860	24359
002P-M-01	Primary Pt.	2	2P	12.975	512.78	1968.4	31284	19223
003P-M-01	Primary Pt.	3	3P	14.05	526.91	2059.6	40753	25042
004P-M-01	Primary Pt.	4	4P	9.068	333.58	1423.0	39616	24147
005P-M-01	Primary Pt.	5	5P	13.675	556.77	2093.2	45182	27638
006P-M-01	Primary Pt.	6	6P	13.237	584.83	1971.2	36990	21636
007P-M-01	Primary Pt.	7	7P	8.357	341.03	1282.3	15779	9619
008P-M-01	Primary Pt.	8	8P	8.851	313.36	1329.5	43476	27032
009D-M-01	Field Dupe	9	9D	23.965	917.75	3442.0	39767	25492
009P-M-01	Primary Pt.	9	9P	24.307	912.48	3207.2	38495	24628
010P-M-01	Primary Pt.	10	10P	16.393	678.10	2493.5	45749	28630
011P-M-01	Primary Pt.	11	11P	6.869	271.07	1105.7	33960	20018
013P-M-01	Primary Pt.	13	13P	9.392	378.51	1454.3	28412	16947
015P-M-01	Primary Pt.	15	15P	2.57	120.82	424.0	6417	3724
016P-M-01	Primary Pt.	16	16P	7.288	350.28	1161.4	25989	15513
017P-M-01	Primary Pt.	17	17P	1.161	47.68	190.6	3024	1896
018D-M-01	Field Dupe	18	18D	1.685	72.80	261.4	7848	4925
018P-M-01	Primary Pt.	18	18P	1.651	69.17	263.6	7793	4896
019P-M-01	Primary Pt.	19	19P	3.184	141.29	518.2	11213	6691
020P-M-01	Primary Pt.	20	20P	5.705	262.98	900.9	10498	6183
021P-M-01	Primary Pt.	21	21P	7.971	292.76	1246.7	22726	13707
022P-M-01	Primary Pt.	22	22P	3.662	147.34	601.9	10461	6266
023P-M-01	Primary Pt.	23	23P	6.162	215.23	980.7	13271	7970
024P-M-01	Primary Pt.	24	24P	6.889	213.05	1136.1	9266	5915
025P-M-01	Primary Pt.	25	25P	5.633	246.32	862.0	15592	9054
026D-M-01	Field Dupe	26	26D	2.582	78.87	420.0	4178	2393
026P-M-01	Primary Pt.	26	26P	1.796	56.04	290.5	2981	1691
028P-M-01	Primary Pt.	28	28P	6.053	226.33	921.9	18108	9972
029P-M-01	Primary Pt.	29	29P	0.516	22.21	119.1	1345	819
030P-M-01	Primary Pt.	30	30P	0.932	37.44	209.2	2641	1803
030R-M-01	Random Dupe	30	30R	0.597	20.89	124.4	1695	1085
031P-M-01	Primary Pt.	31	31P	1.824	62.54	300.6	5377	3479
031R-M-01	Random Dupe	31	31R	2.015	71.83	348.1	6515	4191
032P-M-01	Primary Pt.	32	32P	1.306	55.80	207.5	3906	2318
032R-M-01	Random Dupe	32	32R	1.057	39.11	168.8	3427	2101
033P-M-01	Primary Pt.	33	33P	0.677	21.92	117.3	1019	627
034D-M-01	Field Dupe	34	34D	0.555	18.13	93.6	912	630

Moss Code	Plot Type	Sample Point	Sample No.	Moss Cd (mg/kg dw)	Moss Pb (mg/kg dw)	Moss Zn (mg/kg dw)	Moss Al (mg/kg dw)	Moss Fe (mg/kg dw)
034P-M-01	Primary Pt.	34	34P	0.706	23.38	109.0	1466	956
034R-M-01	Random Dupe	34	34R	0.531	19.58	97.3	1232	841
035P-M-01	Primary Pt.	35	35P	0.537	16.91	92.5	1202	760
036P-M-01	Primary Pt.	36	36P	3.065	110.09	559.3	4929	3348
036R-M-01	Random Dupe	36	36R	2.391	77.64	435.8	3487	2408
037P-M-01	Primary Pt.	37	37P	0.784	25.79	179.4	1179	790
038P-M-01	Primary Pt.	38	38P	0.595	22.26	116.4	1056	657
038R-M-01	Random Dupe	38	38R	0.747	27.55	153.2	1517	1014
039P-M-01	Primary Pt.	39	39P	0.935	44.00	187.5	2750	2171
040P-M-01	Primary Pt.	40	40P	0.521	18.46	72.3	1067	744
040R-M-01	Random Dupe	40	40R	0.381	16.45	71.9	1012	659
041P-M-01	Primary Pt.	41	41P	1.997	56.78	309.4	6672	4461
042D-M-01	Field Dupe	42	42D	0.566	13.82	84.2	917	574
042P-M-01	Primary Pt.	42	42P	0.608	11.11	83.0	740	463
042R-M-01	Random Dupe	42	42R	0.498	13.32	82.9	947	954
044P-M-01	Primary Pt.	44	44P	1.383	39.99	230.0	2200	1561
044R-M-01	Random Dupe	44	44R	1.153	32.64	183.7	1683	1104
045P-M-01	Primary Pt.	45	45P	0.417	15.95	74.4	567	371
046P-M-01	Primary Pt.	46	46P	1.372	49.50	223.0	2344	1452
048P-M-01	Primary Pt.	48	48P	0.797	27.77	129.4	1317	839
048R-M-01	Random Dupe	48	48R	0.956	38.23	147.6	2159	1376
049P-M-01	Primary Pt.	49	49P	0.911	37.38	206.2	787	636
050P-M-01	Primary Pt.	50	50P	2.218	91.21	376.9	1077	825
051A-M-01	Auxiliary Pt.	51	51A	2.173	77.00	357.7	2341	1598
052P-M-01	Primary Pt.	52	52P	3.596	140.55	637.1	5189	3609
053D-M-01	Field Dupe	53	53D	0.915	31.21	196.8	979	677
053P-M-01	Primary Pt.	53	53P	0.826	30.43	193.2	1050	708
054P-M-01	Primary Pt.	54	54P	0.655	21.44	137.4	511	372
055P-M-01	Primary Pt.	55	55P	0.971	37.60	223.7	660	519
056P-M-01	Primary Pt.	56	56P	0.793	22.89	179.2	450	384
057P-M-01	Primary Pt.	57	57P	0.95	42.71	169.9	1006	819
057R-M-01	Random Dupe	57	57R	1.107	54.25	218.3	1341	1068
058P-M-01	Primary Pt.	58	58P	1.828	82.62	319.7	1637	1312
059D-M-01	Field Dupe	59	59D	1.809	70.39	299.5	1633	1319
059P-M-01	Primary Pt.	59	59P	2.301	90.95	383.8	2263	1591
060P-M-01	Primary Pt.	60	60P	1.724	66.32	339.9	2205	1486
061P-M-01	Primary Pt.	61	61P	0.268	3.86	47.7	580	415

Moss Code	Plot Type	Sample Point	Sample No.	Moss Cd (mg/kg dw)	Moss Pb (mg/kg dw)	Moss Zn (mg/kg dw)	Moss Al (mg/kg dw)	Moss Fe (mg/kg dw)
061R-M-01	Random Dupe	61	61R	0.16	4.53	55.1	566	421
062P-M-01	Primary Pt.	62	62P	0.446	13.16	81.6	1159	796
062R-M-01	Random Dupe	62	62R	0.417	3.50	75.3	343	262
063D-M-01	Field Dupe	63	63D	0.315	4.56	43.6	800	412
063P-M-01	Primary Pt.	63	63P	0.208	4.48	38.6	635	385
064P-M-01	Primary Pt.	64	64P	0.171	3.92	41.2	513	386
064R-M-01	Random Dupe	64	64R	0.141	3.53	42.0	518	404
065P-M-01	Primary Pt.	65	65P	0.27	1.96	42.4	617	460
065R-M-01	Random Dupe	65	65R	0.159	2.74	38.1	995	751
066D-M-01	Field Dupe	66	66D	0.463	1.78	46.1	360	299
066P-M-01	Primary Pt.	66	66P	0.658	2.29	56.6	432	340
066R-M-01	Random Dupe	66	66R	0.318	3.54	45.1	477	377
067P-M-01	Primary Pt.	67	67P	0.124	1.78	34.3	383	260
067R-M-01	Random Dupe	67	67R	0.137	2.42	30.7	633	458
068P-M-01	Primary Pt.	68	68P	0.127	5.09	46.0	399	332
068R-M-01	Random Dupe	68	68R	0.12	4.47	42.9	265	308
069P-M-01	Primary Pt.	69	69P	0.299	5.79	36.9	512	335
070P-M-01	Primary Pt.	70	70P	0.22	6.50	75.3	531	372
070R-M-01	Random Dupe	70	70R	0.228	6.73	47.1	550	378
071P-M-01	Primary Pt.	71	71P	0.231	5.04	60.0	403	298
071R-M-01	Random Dupe	71	71R	0.258	3.89	63.3	941	634
072P-M-01	Primary Pt.	72	72P	0.613	7.98	56.1	926	547
073P-M-01	Primary Pt.	73	73P	0.297	3.96	57.2	410	289
073R-M-01	Random Dupe	73	73R	0.325	3.26	50.7	353	248
074P-M-01	Primary Pt.	74	74P	0.188	3.41	37.8	760	442
075P-M-01	Primary Pt.	75	75P	0.128	4.24	35.5	541	366
076P-M-01	Primary Pt.	76	76P	0.258	9.02	54.1	1412	806
076R-M-01	Random Dupe	76	76R	0.156	3.89	40.7	1606	757
077P-M-01	Primary Pt.	77	77P	0.343	4.98	50.8	495	358
078P-M-01	Primary Pt.	78	78P	0.223	5.81	53.2	551	410
079P-M-01	Primary Pt.	79	79P	0.242	5.48	95.8	641	426
079R-M-01	Random Dupe	79	79R	0.333	3.49	42.1	341	251
080P-M-01	Primary Pt.	80	80P	0.192	5.50	36.8	556	475
080R-M-01	Random Dupe	80	80R	0.145	4.89	36.3	491	382
081P-M-01	Primary Pt.	81	81P	0.308	10.19	71.7	589	441
082P-M-01	Primary Pt.	82	82P	0.236	3.62	41.8	287	237
082R-M-01	Random Dupe	82	82R	0.424	8.79	63.1	1474	1040

Moss Code	Plot Type	Sample Point	Sample No.	Moss Cd (mg/kg dw)	Moss Pb (mg/kg dw)	Moss Zn (mg/kg dw)	Moss Al (mg/kg dw)	Moss Fe (mg/kg dw)
083P-M-01	Primary Pt.	83	83P	0.247	8.16	62.3	830	537
083R-M-01	Random Dupe	83	83R	0.298	10.56	59.5	764	502
084P-M-01	Primary Pt.	84	84P	0.318	4.20	77.7	416	236
085P-M-01	Primary Pt.	85	85P	0.272	9.17	110.6	547	380
085R-M-01	Random Dupe	85	85R	0.362	7.34	77.8	483	339
086P-M-01	Primary Pt.	86	86P	0.783	7.16	52.8	2303	1105
087P-M-01	Primary Pt.	87	87P	0.277	5.52	43.9	348	256
087R-M-01	Random Dupe	87	87R	0.286	7.45	71.2	431	317
088P-M-01	Primary Pt.	88	88P	0.303	6.24	54.2	422	325
088R-M-01	Random Dupe	88	88R	0.395	7.72	72.8	749	635
089A-M-01	Auxiliary Pt.	89	89A	0.18	7.47	53.3	396	293
089R-M-01	Random Dupe	89	89R	0.247	6.30	44.9	362	269
090P-M-01	Primary Pt.	90	90P	0.343	13.72	63.8	625	477
090R-M-01	Random Dupe	90	90R	0.455	14.72	59.0	558	433
091P-M-01	Primary Pt.	91	91P	0.296	11.52	52.5	481	375
091R-M-01	Random Dupe	91	91R	0.249	8.25	43.1	470	381
092P-M-01	Primary Pt.	92	92P	0.382	6.40	39.2	409	426
093P-M-01	Primary Pt.	93	93P	0.409	11.56	57.1	501	370
094P-M-01	Primary Pt.	94	94P	0.246	6.18	39.2	491	295
094R-M-01	Random Dupe	94	94R	0.161	3.03	38.5	323	268
095P-M-01	Primary Pt.	95	95P	0.264	6.00	44.0	1141	786
097P-M-01	Primary Pt.	97	97P	0.744	23.10	197.3	648	456
097R-M-01	Random Dupe	97	97R	0.856	27.08	177.5	603	457
098P-M-01	Primary Pt.	98	98P	0.598	17.01	77.7	1733	1149
099D-M-01	Field Dupe	99	99D	0.377	6.43	84.8	475	320
099P-M-01	Primary Pt.	99	99P	0.341	7.55	89.3	430	317
099R-M-01	Random Dupe	99	99R	0.618	8.95	85.6	560	403
100A-M-01	Auxiliary Pt.	100	100A	0.448	17.06	83.4	793	626
101P-M-01	Primary Pt.	101	101P	0.563	12.73	79.9	822	560
102P-M-01	Primary Pt.	102	102P	0.849	29.11	140.8	1933	1343
103P-M-01	Primary Pt.	103	103P	0.453	11.85	85.6	15015	10051
104P-M-01	Primary Pt.	104	104P	0.509	15.40	72.5	693	506
105P-M-01	Primary Pt.	105	105P	0.387	14.70	95.7	724	537
105R-M-01	Random Dupe	105	105R	0.295	9.76	63.2	589	420
106P-M-01	Primary Pt.	106	106P	0.532	16.21	67.4	665	501
107P-M-01	Primary Pt.	107	107P	0.462	16.89	91.2	608	456
107R-M-01	Random Dupe	107	107R	0.328	14.86	87.1	404	334

Moss Code	Plot Type	Sample Point	Sample No.	Moss Cd (mg/kg dw)	Moss Pb (mg/kg dw)	Moss Zn (mg/kg dw)	Moss Al (mg/kg dw)	Moss Fe (mg/kg dw)
108P-M-01	Primary Pt.	108	108P	0.885	32.35	146.9	684	692
109A-M-01	Auxiliary Pt.	109	109A	0.408	10.79	92.3	431	342
109R-M-01	Random Dupe	109	109R	0.497	17.30	95.9	567	438
110P-M-01	Primary Pt.	110	110P	0.711	25.09	134.3	1047	732
111P-M-01	Primary Pt.	111	111P	0.472	19.30	141.4	1433	963
112P-M-01	Primary Pt.	112	112P	0.329	11.80	66.9	2078	1947
112R-M-01	Random Dupe	112	112R	0.379	15.73	71.2	599	520
113P-M-01	Primary Pt.	113	113P	0.548	16.83	107.0	1832	1527
114P-M-01	Primary Pt.	114	114P	0.566	22.44	88.3	773	602
114R-M-01	Random Dupe	114	114R	0.438	14.41	72.6	563	436
115P-M-01	Primary Pt.	115	115P	0.44	11.95	75.8	761	587
116P-M-01	Primary Pt.	116	116P	0.554	14.11	87.8	594	552
117P-M-01	Primary Pt.	117	117P	0.626	22.05	101.2	1299	880
117R-M-01	Random Dupe	117	117R	0.786	26.97	118.5	961	734
118P-M-01	Primary Pt.	118	118P	0.668	20.36	132.9	1065	1062
119P-M-01	Primary Pt.	119	119P	0.76	20.51	122.9	12906	9182
119R-M-01	Random Dupe	119	119R	0.724	18.37	113.3	12489	8837
120P-M-01	Primary Pt.	120	120P	0.906	35.42	155.6	2432	2532
121A-M-01	Auxiliary Pt.	121	121A	0.455	12.22	66.7	887	629
122A-M-01	Auxiliary Pt.	122	122A	0.634	17.84	99.7	3991	2924
122R-M-01	Random Dupe	122	122R	1.198	10.98	120.6	706	493
123P-M-01	Primary Pt.	123	123P	0.378	11.02	59.8	556	516
124P-M-01	Primary Pt.	124	124P	0.338	11.81	60.5	450	338
124R-M-01	Random Dupe	124	124R	0.383	9.96	51.9	303	226
125P-M-01	Primary Pt.	125	125P	0.349	13.72	63.9	379	313
126P-M-01	Primary Pt.	126	126P	0.415	14.52	80.1	536	389
127P-M-01	Primary Pt.	127	127P	0.462	13.90	83.1	540	580
127R-M-01	Random Dupe	127	127R	0.53	15.15	77.5	523	405
136P-M-01	Primary Pt.	136	136P	0.144	1.72	45.8	349	268
137P-M-01	Primary Pt.	137	137P	0.224	1.13	37.1	430	193
138P-M-01	Primary Pt.	138	138P	0.088	1.42	24.6	373	257
138R-M-01	Random Dupe	138	138R	0.146	1.44	41.8	341	237
139P-M-01	Primary Pt.	139	139P	0.132	1.69	56.6	735	527
140A-M-01	Auxiliary Pt.	140	140A	0.169	2.13	56.0	355	268
140R-M-01	Random Dupe	140	140R	0.131	1.94	38.2	368	264
141A-M-01	Auxiliary Pt.	141	141A	0.125	1.51	46.2	596	405
141D-M-01	Field Dupe	141	141D	0.12	1.71	38.5	710	473

Moss Code	Plot Type	Sample Point	Sample No.	Moss Cd (mg/kg dw)	Moss Pb (mg/kg dw)	Moss Zn (mg/kg dw)	Moss Al (mg/kg dw)	Moss Fe (mg/kg dw)
141R-M-01	Random Dupe	141	141R	0.088	1.53	29.0	534	368
142P-M-01	Primary Pt.	142	142P	0.153	2.30	38.0	346	251
142R-M-01	Random Dupe	142	142R	0.164	2.12	35.8	342	290
143P-M-01	Primary Pt.	143	143P	0.159	2.51	41.2	397	329
144P-M-01	Primary Pt.	144	144P	0.263	2.10	80.9	489	387
145P-M-01	Primary Pt.	145	145P	0.189	3.45	46.7	436	347
145R-M-01	Random Dupe	145	145R	0.187	3.44	66.6	403	327
146P-M-01	Primary Pt.	146	146P	0.528	17.33	59.5	337	259
146R-M-01	Random Dupe	146	146R	0.357	10.39	60.0	292	255
147A-M-01	Auxiliary Pt.	147	147A	0.703	17.20	100.4	911	663
148D-M-01	Field Dupe	148	148D	0.65	23.49	83.5	374	350
148P-M-01	Primary Pt.	148	148P	0.677	23.91	102.0	398	308
148R-M-01	Random Dupe	148	148R	0.536	18.66	84.0	520	398
149P-M-01	Primary Pt.	149	149P	0.791	41.77	122.3	499	408
150P-M-01	Primary Pt.	150	150P	0.266	9.60	99.1	640	461
151P-M-01	Primary Pt.	151	151P	0.238	7.43	69.1	3723	2775
151R-M-01	Random Dupe	151	151R	0.339	13.39	65.4	471	351
152P-M-01	Primary Pt.	152	152P	0.547	22.62	82.2	362	334
153P-M-01	Primary Pt.	153	153P	0.307	6.66	71.3	2059	1651
154P-M-01	Primary Pt.	154	154P	0.647	18.47	92.8	411	344
155P-M-01	Primary Pt.	155	155P	0.352	6.83	93.3	407	301
155R-M-01	Random Dupe	155	155R	0.304	7.28	89.6	353	265
156D-M-01	Field Dupe	156	156D	0.259	5.89	54.9	271	204
156P-M-01	Primary Pt.	156	156P	0.286	5.95	69.9	225	168
156R-M-01	Random Dupe	156	156R	0.261	4.45	74.3	232	179
157P-M-01	Primary Pt.	157	157P	0.183	2.88	62.7	540	374
157R-M-01	Random Dupe	157	157R	0.221	38.62	58.5	485	343
159P-M-01	Primary Pt.	159	159P	0.576	6.57	64.7	1674	1193
159R-M-01	Random Dupe	159	159R	1.086	2.30	115.0	360	322
160P-M-01	Primary Pt.	160	160P	0.187	6.60	44.5	356	265
160R-M-01	Random Dupe	160	160R	0.157	3.04	52.3	478	318
161P-M-01	Primary Pt.	161	161P	0.682	21.55	128.5	791	557
161R-M-01	Random Dupe	161	161R	0.679	23.95	155.6	858	607
162P-M-01	Primary Pt.	162	162P	0.604	19.84	156.9	408	337
162R-M-01	Random Dupe	162	162R	0.602	20.60	133.3	418	326
163P-M-01	Primary Pt.	163	163P	0.67	24.96	108.7	828	793
163R-M-01	Random Dupe	163	163R	0.644	23.54	121.3	809	673

Moss Code	Plot Type	Sample Point	Sample No.	Moss Cd (mg/kg dw)	Moss Pb (mg/kg dw)	Moss Zn (mg/kg dw)	Moss Al (mg/kg dw)	Moss Fe (mg/kg dw)
164P-M-01	Primary Pt.	164	164P	0.625	23.29	120.2	382	330
170P-M-01	Primary Pt.	170	170P	0.124	1.29	35.3	236	202
170R-M-01	Random Dupe	170	170R	0.141	1.59	35.0	409	313
171P-M-01	Primary Pt.	171	171P	0.22	2.84	36.1	385	305
201P-M-01	Off-grid	201	201O	0.761	15.49	132.4	706	518
202P-M-01	Off-grid	202	202O	0.421	10.54	66.1	401	312
203P-M-01	Off-grid	203	203O	0.478	11.81	105.2	1051	723

APPENDIX II

SOIL DATA

Soil Code	Plot Type	Sample Point	Sample No.	Soil Cd (mg/kg dw)	Soil Pb (mg/kg dw)	Soil Zn (mg/kg dw)	Soil Al (mg/kg dw)	Soil Fe (mg/kg dw)
54P-S-01	Primary Pt.	54	54P	0.170	15.20	90.8	60000	30700
55P-S-01	Primary Pt.	55	55P	0.157	10.20	61.4	42300	22300
57P-S-01	Primary Pt.	57	57P	0.309	13.70	86.6	52300	43900
59P-S-01	Primary Pt.	59	59P	0.214	12.60	75.5	60200	47500
64P-S-01	Primary Pt.	64	64P	0.279	11.00	74.5	59800	26200
91P-S-01	Primary Pt.	91	91P	0.301	16.10	103.0	65900	43500
99P-S-01	Primary Pt.	99	99P	0.299	83.80	129.0	63000	40600
115P-S-01	Primary Pt.	115	115P	0.277	16.50	112.0	70300	49000
119P-S-01	Primary Pt.	119	119P	0.285	7.80	95.9	25900	27200
123P-S-01	Primary Pt.	123	123P	0.177	17.90	83.7	69600	38200
136P-S-01	Primary Pt.	136	136P	0.290	10.90	67.5	56400	26100
138P-S-01	Primary Pt.	138	138P	0.088	8.09	76.8	74600	35900
139P-S-01	Primary Pt.	139	139P	0.746	14.40	153.0	83000	40600
141A-S-01	Auxillary Pt.	141	141A	0.405	14.70	118.0	70600	42500
142P-S-01	Primary Pt.	142	142P	0.160	11.50	80.9	58000	38900
143P-S-01	Primary Pt.	143	143P	0.270	12.30	105.0	63200	41800
144P-S-01	Primary Pt.	144	144P	0.281	14.80	105.0	67600	49800
145P-S-01	Primary Pt.	145	145P	0.477	16.70	125.0	73000	47500
147A-S-01	Auxillary Pt.	147	147A	0.550	32.70	164.0	57800	32600
148D-S-01	Random Dupe	148	148D	0.248	18.70	102.0	57800	38500
148P-S-01	Primary Pt.	148	148P	0.243	20.10	110.0	62900	44300
149P-S-01	Primary Pt.	149	149P	0.515	12.50	75.5	46000	35400
151P-S-01	Primary Pt.	151	151P	0.131	15.50	79.6	68300	40400
152P-S-01	Primary Pt.	152	152P	0.175	16.30	72.2	48900	29900
154P-S-01	Primary Pt.	154	154P	0.282	15.90	83.1	51200	38200
155P-S-01	Primary Pt.	155	155P	0.341	10.70	101.0	45800	38900
157P-S-01	Primary Pt.	157	157P	0.209	18.80	117.0	86600	46900
160P-S-01	Primary Pt.	160	160P	0.0828	14.90	84.1	70600	39100
161P-S-01	Primary Pt.	161	161P	0.226	10.70	108.0	56800	31900
170P-S-01	Primary Pt.	170	170P	0.197	13.10	89.9	61400	43900
5P-S-01	Primary Pt.	5	5P	0.265	15.00	70.2	50300	24900
45P-S-01	Primary Pt.	45	45P	0.343	25.90	103.0	69300	67000
52P-S-01	Primary Pt.	52	52P	0.336	13.10	118.0	52700	32000
61P-S-01	Primary Pt.	61	61P	0.0693	41.60	99.1	78900	51400
62P-S-01	Primary Pt.	62	62P	0.244	14.20	96.6	62600	45700
82P-S-01	Primary Pt.	82	82P	0.321	18.30	96.9	61400	40400
93P-S-01	Primary Pt.	93	93P	0.212	16.60	109.0	63600	44000

Soil Code	Plot Type	Sample Point	Sample No.	Soil Cd (mg/kg dw)	Soil Pb (mg/kg dw)	Soil Zn (mg/kg dw)	Soil Al (mg/kg dw)	Soil Fe (mg/kg dw)
109A-S-01	Auxillary Pt.	109	109A	0.295	18.30	132.0	61300	69500
113P-S-01	Primary Pt.	113	113P	0.176	17.80	94.2	53800	44400
124P-S-01	Primary Pt.	124	124P	0.291	23.60	118.0	71200	71800
1P-S-01	Primary Pt.	1	1P	0.454	30.50	133.0	77500	58200
3P-S-01	Primary Pt.	3	3P	0.149	15.80	51.6	49900	15100
6P-S-01	Primary Pt.	6	6P	0.353	15.70	70.2	52600	21400
11P-S-01	Primary Pt.	11	11P	0.172	17.70	102.0	65100	38000
16P-S-01	Primary Pt.	16	16P	0.177	13.60	60.5	50100	19200
21P-S-01	Primary Pt.	21	21P	0.152	12.40	49.0	44900	14400

APPENDIX III

SITE DATA

Moss Code	Plot Type	Sample Point	Sample No.	Stratum	Latitude	Longitude	Side of Road	Aspect (deg)	Slope	Elev (m)	Viereck Veg type
001P-M-01	Primary Pt.	1	1P	1	67.66545	-163.71411	N	0	0	150	II.C.2.a
002P-M-01	Primary Pt.	2	2P	1	67.65547	-163.75245	N	0	0	162	II.C.2.a
003P-M-01	Primary Pt.	3	3P	1	67.64303	-163.79069	N	0	0	166	II.C.2.a
004P-M-01	Primary Pt.	4	4P	1	67.68825	-163.67952	N	0	0	167	II.C.2.a
005P-M-01	Primary Pt.	5	5P	1	67.6344	-163.83046	N	0	0	128	II.C.2.a
006P-M-01	Primary Pt.	6	6P	1	67.62779	-163.87078	S	360	1	123	II.C.2.a
007P-M-01	Primary Pt.	7	7P	1	67.76497	-163.53371	N	0	0	187	II.C.2.a
008P-M-01	Primary Pt.	8	8P	1	67.72111	-163.64955	N	0	0	119	II.C.2.a
009D-M-01	Field Dupe	9	9D	1	67.6024	-163.94707	N	0	0	67	II.C.2.a
009P-M-01	Primary Pt.	9	9P	1	67.6024	-163.94707	N	0	0	67	II.C.2.a
010P-M-01	Primary Pt.	10	10P	1	67.62083	-163.91041	N	0	0	98	II.C.2.a
011P-M-01	Primary Pt.	11	11P	1	67.74294	-163.61551	N	104	2	164	II.C.1.b
013P-M-01	Primary Pt.	13	13P	1	67.76647	-163.57866	N	0	0	166	II.C.2.a
015P-M-01	Primary Pt.	15	15P	2	67.64413	-163.76838	S	54	5	167	II.C.2.a
016P-M-01	Primary Pt.	16	16P	2	67.66281	-163.73255	S	0	0	162	II.C.2.a
017P-M-01	Primary Pt.	17	17P	2	67.678	-163.69575	S	230	1	176	II.C.2.a
018D-M-01	Field Dupe	18	18D	2	67.63651	-163.80837	S	240	3	167	II.C.2.a
018P-M-01	Primary Pt.	18	18P	2	67.63651	-163.80837	S	240	3	167	II.C.2.a
019P-M-01	Primary Pt.	19	19P	2	67.7004	-163.66173	S	360	1	159	II.C.2.a
020P-M-01	Primary Pt.	20	20P	2	67.63252	-163.84987	N	42	5	113	II.C.2.a
021P-M-01	Primary Pt.	21	21P	2	67.62473	-163.88989	S	306	3	108	II.C.2.a
022P-M-01	Primary Pt.	22	22P	2	67.73035	-163.63042	N	144	8	133	II.C.2.a
023P-M-01	Primary Pt.	23	23P	2	67.77612	-163.51631	S	0	0	182	II.C.2.a
024P-M-01	Primary Pt.	24	24P	2	67.6019	-163.95564	N	330	1	63	II.C.2.a
025P-M-01	Primary Pt.	25	25P	2	67.61345	-163.92834	N	0	0	83	II.C.2.a
026D-M-01	Field Dupe	26	26D	2	67.76849	-163.55630	N	268	4	165	II.C.2.a
026P-M-01	Primary Pt.	26	26P	2	67.76849	-163.55630	N	268	4	165	II.C.2.a
028P-M-01	Primary Pt.	28	28P	2	67.76385	-163.60090	S	0	0	161	II.C.2.a
029P-M-01	Primary Pt.	29	29P	3	67.62794	-163.81546	S	0	0	134	II.C.2.a
030P-M-01	Primary Pt.	30	30P	3	67.63476	-163.79880	S	0	0	173	II.C.2.a
030R-M-01	Random Dupe	30	30R	3	67.63448	-163.79897	S	0	0	171	II.C.2.a
031P-M-01	Primary Pt.	31	31P	3	67.66549	-163.73335	N	360	1	153	II.C.2.a
031R-M-01	Random Dupe	31	31R	3	67.66514	-163.73381	N	360	1	153	II.C.2.a
032P-M-01	Primary Pt.	32	32P	3	67.67725	-163.71429	N	206	4	153	II.C.2.a
032R-M-01	Random Dupe	32	32R	3	67.67732	-163.71390	N	206	4	151	II.C.2.a
033P-M-01	Primary Pt.	33	33P	3	67.66936	-163.68859	S	201	3	167	II.C.2.a
034D-M-01	Field Dupe	34	34D	3	67.67252	-163.68258	S	0	0	167	II.C.2.a

Moss Code	Plot Type	Sample Point	Sample No.	Stratum	Latitude	Longitude	Side of Road	Aspect (deg)	Slope	Elev (m)	Viereck Veg type
034P-M-01	Primary Pt.	34	34P	3	67.67252	-163.68258	S	0	0	167	II.C.2.a
034R-M-01	Random Dupe	34	34R	3	67.67264	-163.68327	S	0	0	167	
035P-M-01	Primary Pt.	35	35P	3	67.69331	-163.64781	S	260	4	194	II.C.2.a
036P-M-01	Primary Pt.	36	36P	3	67.60609	-163.96098	N	0	0	62	II.C.2.a
036R-M-01	Random Dupe	36	36R	3	67.60636	-163.96105	N	0	0	62	
037P-M-01	Primary Pt.	37	37P	3	67.60353	-163.91596	S	340	4	90	II.C.2.a
038P-M-01	Primary Pt.	38	38P	3	67.61521	-163.89278	S	295	1	116	II.C.2.a
038R-M-01	Random Dupe	38	38R	3	67.6154	-163.89290	S	295	1	119	
039P-M-01	Primary Pt.	39	39P	3	67.68635	-163.71144	N	364	1	167	II.C.2.a
040P-M-01	Primary Pt.	40	40P	3	67.7141	-163.63913	S	20	1	152	II.C.2.a
040R-M-01	Random Dupe	40	40R	3	67.71417	-163.63833	S	20	1	151	
041P-M-01	Primary Pt.	41	41P	3	67.73685	-163.62595	N	204	4	146	READ ME
042D-M-01	Field Dupe	42	42D	3	67.72952	-163.60721	S	334	3	127	II.B.2.a
042P-M-01	Primary Pt.	42	42P	3	67.72952	-163.60721	S	334	3	127	II.B.2.a
042R-M-01	Random Dupe	42	42R	3	67.72895	-163.60670	S	334	3	127	
044P-M-01	Primary Pt.	44	44P	3	67.76208	-163.54177	S	322	2	166	II.C.2.a
044R-M-01	Random Dupe	44	44R	3	67.76214	-163.54164	S	322	2	167	
045P-M-01	Primary Pt.	45	45P	3	67.7715	-163.50647	S	0	0	200	II.C.2.a
046P-M-01	Primary Pt.	46	46P	3	67.75225	-163.62973	N	107	2	198	II.C.2.a
048P-M-01	Primary Pt.	48	48P	3	67.77249	-163.58293	N	270	0.5	160	II.C.2.a
048R-M-01	Random Dupe	48	48R	3	67.77219	-163.58270	N	270	0.5	159	
049P-M-01	Primary Pt.	49	49P	4	67.61727	-164.08043	N	0	0	22	II.C.2.a
050P-M-01	Primary Pt.	50	50P	4	67.6028	-164.06755	N	350	1	25	II.C.2.a
051A-M-01	Auxillary Pt.	51	51A	4	67.60278	-164.02040	N	20	3	53	II.C.2.a
052P-M-01	Primary Pt.	52	52P	4	67.60369	-163.99327	N	196	2	47	II.C.2.a
053D-M-01	Field Dupe	53	53D	4	67.58382	-163.95947	S	265	4	80	II.C.2.a
053P-M-01	Primary Pt.	53	53P	4	67.58382	-163.95947	S	265	4	80	II.C.2.a
054P-M-01	Primary Pt.	54	54P	4	67.57075	-163.96007	S	240	2	63	II.C.2.a
055P-M-01	Primary Pt.	55	55P	4	67.55877	-163.98061	S	0	0	31	II.C.2.a
056P-M-01	Primary Pt.	56	56P	4	67.55275	-163.99665	S	248	1	19	II.C.2.a
057P-M-01	Primary Pt.	57	57P	5	67.61924	-164.08005	N	0	0	17	II.C.2.a
057R-M-01	Random Dupe	57	57R	5	67.61918	-164.08036	N	0	0	17	
058P-M-01	Primary Pt.	58	58P	5	67.60976	-164.04862	N	342	1	23	II.C.2.a
059D-M-01	Field Dupe	59	59D	5	67.60651	-164.03325	N	2	5	38	II.C.2.a
059P-M-01	Primary Pt.	59	59P	5	67.60651	-164.03325	N	2	5	38	II.C.2.a
060P-M-01	Primary Pt.	60	60P	5	67.60515	-163.98076	N	348	3	44	II.C.2.a
061P-M-01	Primary Pt.	61	61P	6	67.51025	-163.65534	S	270	4	141	II.C.2.a

Moss Code	Plot Type	Sample Point	Sample No.	Stratum	Latitude	Longitude	Side of Road	Aspect (deg)	Slope	Elev (m)	Viereck Veg type
061R-M-01	Random Dupe	61	61R	6	67.51102	-163.65613	S	20	7	138	
062P-M-01	Primary Pt.	62	62P	6	67.56617	-163.53741	S	194	7	170	II.C.2.a
062R-M-01	Random Dupe	62	62R	6	67.5665	-163.53733	S	194	7	173	
063D-M-01	Field Dupe	63	63D	6	67.60066	-163.46931	S	234	6	176	II.C.2.c
063P-M-01	Primary Pt.	63	63P	6	67.60066	-163.46931	S	234	6	176	II.C.2.c
064P-M-01	Primary Pt.	64	64P	6	67.58496	-163.42242	S	244	1	139	II.C.2.a
064R-M-01	Random Dupe	64	64R	6	67.58501	-163.42175	S	244	1	136	
065P-M-01	Primary Pt.	65	65P	6	67.64361	-163.31748	S	362	2	267	II.B.2.a
065R-M-01	Random Dupe	65	65R	6	67.64357	-163.31795	S	362	1	267	
066D-M-01	Field Dupe	66	66D	6	67.65197	-163.28803	S	212	4	267	II.C.1.b
066P-M-01	Primary Pt.	66	66P	6	67.65197	-163.28803	S	212	4	267	II.C.1.b
066R-M-01	Random Dupe	66	66R	6	67.65149	-163.28771	S	212	3	273	II.C.2.a
067P-M-01	Primary Pt.	67	67P	6	67.66379	-163.26952	S	110	2	326	MIXED
067R-M-01	Random Dupe	67	67R	6	67.66363	-163.26955	S	110	2	323	
068P-M-01	Primary Pt.	68	68P	6	67.46914	-163.87233	S	0	0	12	II.C.2.a
068R-M-01	Random Dupe	68	68R	6	67.46947	-163.87284	S	0	0	12	
069P-M-01	Primary Pt.	69	69P	6	67.51982	-163.81720	S	287	0	252	II.D.1
070P-M-01	Primary Pt.	70	70P	6	67.53873	-163.77664	S	26	2	139	II.C.2.a
070R-M-01	Random Dupe	70	70R	6	67.53849	-163.77588	S	26	3	137	
071P-M-01	Primary Pt.	71	71P	6	67.51559	-163.71709	S	300	6	161	II.C.2.a
071R-M-01	Random Dupe	71	71R	6	67.51573	-163.71666	S	300	6	161	
072P-M-01	Primary Pt.	72	72P	6	67.56407	-163.66347	S	271	35	271	II.C.2.c
073P-M-01	Primary Pt.	73	73P	6	67.57013	-163.62334	S	360	15	165	II.C.2.a
073R-M-01	Random Dupe	73	73R	6	67.56986	-163.62191	S	360	15	171	
074P-M-01	Primary Pt.	74	74P	6	67.57593	-163.60847	S	199	15	170	II.B.1.a
075P-M-01	Primary Pt.	75	75P	6	67.59028	-163.52173	S	220	5	259	II.C.2.c
076P-M-01	Primary Pt.	76	76P	6	67.62137	-163.48876	S	260	10	259	MIXED
076R-M-01	Random Dupe	76	76R	6	67.62119	-163.48969	S	260	10	251	
077P-M-01	Primary Pt.	77	77P	6	67.64774	-163.45136	S	339	5	277	II.B.1.a
078P-M-01	Primary Pt.	78	78P	6	67.68721	-163.42654	S	320	3	302	II.C.2.a
079P-M-01	Primary Pt.	79	79P	6	67.69772	-163.36314	S	130	7	220	II.C.1.b
079R-M-01	Random Dupe	79	79R	6	67.69798	-163.36423	S	130	7	223	
080P-M-01	Primary Pt.	80	80P	6	67.68998	-163.32474	S	327	1	253	II.C.2.a
080R-M-01	Random Dupe	80	80R	6	67.69001	-163.32501	S	327	1	253	
081P-M-01	Primary Pt.	81	81P	6	67.53972	-163.92680	S	208	3	63	II.C.2.a
082P-M-01	Primary Pt.	82	82P	6	67.52801	-163.88197	S	239	2	66	II.C.2.a
082R-M-01	Random Dupe	82	82R	6	67.52817	-163.88308	S	239	2	63	

Moss Code	Plot Type	Sample Point	Sample No.	Stratum	Latitude	Longitude	Side of Road	Aspect (deg)	Slope	Elev (m)	Viereck Veg type
083P-M-01	Primary Pt.	83	83P	6	67.56518	-163.83257	S	264	14	189	II.C.2.a
083R-M-01	Random Dupe	83	83R	6	67.56518	-163.83144	S	264	14	195	
084P-M-01	Primary Pt.	84	84P	6	67.54917	-163.81714	S	188	7	124	II.C.2.a
085P-M-01	Primary Pt.	85	85P	6	67.62514	-163.75076	S	250	5	244	II.C.2.a
085R-M-01	Random Dupe	85	85R	6	67.62484	-163.75067	S	250	3	260	
086P-M-01	Primary Pt.	86	86P	6	67.5999	-163.69965	S	200	15	398	READ ME
087P-M-01	Primary Pt.	87	87P	6	67.64663	-163.64639	S	24	5	178	II.C.1.b
087R-M-01	Random Dupe	87	87R	6	67.64671	-163.64692	S	22	5	178	
088P-M-01	Primary Pt.	88	88P	6	67.63825	-163.63437	S	50	5	195	II.C.1.b
088R-M-01	Random Dupe	88	88R	6	67.63824	-163.63263	S	137	6	202	
089A-M-01	Auxiliary Pt.	89	89A	6	67.68161	-163.58387	S	80	15	289	II.C.2.a
089R-M-01	Random Dupe	89	89R	6	67.68142	-163.58378	S	80	15	287	
090P-M-01	Primary Pt.	90	90P	6	67.7148	-163.51836	S	311	8	184	II.C.2.a
090R-M-01	Random Dupe	90	90R	6	67.71524	-163.51844	S	311	8	189	
091P-M-01	Primary Pt.	91	91P	6	67.70098	-163.46143	S	252	7	181	II.C.2.a
091R-M-01	Random Dupe	91	91R	6	67.70122	-163.46192	S	252	7	174	
092P-M-01	Primary Pt.	92	92P	6	67.73064	-163.42493	S	300	1	169	II.C.2.a
093P-M-01	Primary Pt.	93	93P	6	67.76348	-163.38204	S	320	3	284	II.C.2.a
094P-M-01	Primary Pt.	94	94P	6	67.75906	-163.33999	S	266	3	209	II.B.1.a
094R-M-01	Random Dupe	94	94R	6	67.75894	-163.34073	S	266	4	206	
095P-M-01	Primary Pt.	95	95P	6	67.75349	-163.28686	S	235	4	244	II.C.2.a
097P-M-01	Primary Pt.	97	97P	6	67.56482	-163.94792	S	240	4	68	II.C.2.a
097R-M-01	Random Dupe	97	97R	6	67.56504	-163.94837	S	240	4	68	
098P-M-01	Primary Pt.	98	98P	6	67.59204	-163.88981	S	200	3	187	II.D.2
099D-M-01	Field Dupe	99	99D	6	67.60981	-163.80415	S	270	9	194	II.C.2.a
099P-M-01	Primary Pt.	99	99P	6	67.60981	-163.80415	S	270	9	194	II.C.2.a
099R-M-01	Random Dupe	99	99R	6	67.61	-163.80367	S	300	7	192	
100A-M-01	Auxiliary Pt.	100	100A	6	67.70404	-163.78004	N	66	1	134	II.C.2.a
101P-M-01	Primary Pt.	101	101P	6	67.68754	-163.74731	N	191	2	160	II.C.2.a
102P-M-01	Primary Pt.	102	102P	6	67.70752	-163.68727	N	0	0	130	II.C.2.a
103P-M-01	Primary Pt.	103	103P	6	67.72047	-163.60221	S	218	3	101	II.C.2.a
104P-M-01	Primary Pt.	104	104P	6	67.73795	-163.53132	S	308	6	154	II.B.2.a
105P-M-01	Primary Pt.	105	105P	6	67.73299	-163.50581	S	146	7	205	II.C.2.a
105R-M-01	Random Dupe	105	105R	6	67.73294	-163.50705	S	146	7	206	
106P-M-01	Primary Pt.	106	106P	6	67.75835	-163.45471	S	310	2	237	II.C.2.a
107P-M-01	Primary Pt.	107	107P	6	67.77372	-163.39252	S	300	2	246	II.C.2.a
107R-M-01	Random Dupe	107	107R	6	67.77395	-163.39305	S	300	2	246	

Moss Code	Plot Type	Sample Point	Sample No.	Stratum	Latitude	Longitude	Side of Road	Aspect (deg)	Slope	Elev (m)	Viereck Veg type
108P-M-01	Primary Pt.	108	108P	6	67.62057	-164.06872	N	0	0	28	II.C.2.a
109A-M-01	Auxillary Pt.	109	109A	6	67.64064	-164.02779	N	360	1	38	II.C.2.a
109R-M-01	Random Dupe	109	109R	6	67.6406	-164.02735	N	360	1	40	
110P-M-01	Primary Pt.	110	110P	6	67.62312	-163.96780	N	168	1	81	II.C.2.a
111P-M-01	Primary Pt.	111	111P	6	67.65412	-163.86865	N	0	0	101	II.C.2.a
112P-M-01	Primary Pt.	112	112P	6	67.70075	-163.87825	N	339	3	84	II.C.2.a
112R-M-01	Random Dupe	112	112R	6	67.70102	-163.87651	N	300	3	85	
113P-M-01	Primary Pt.	113	113P	6	67.68982	-163.77885	N	0	0	156	II.C.2.a
114P-M-01	Primary Pt.	114	114P	6	67.74456	-163.76766	N	260	3	119	II.C.2.a
114R-M-01	Random Dupe	114	114R	6	67.74522	-163.76699	N	286	3	118	
115P-M-01	Primary Pt.	115	115P	6	67.73114	-163.72426	N	111	1	125	II.C.2.a
116P-M-01	Primary Pt.	116	116P	6	67.76766	-163.65072	N	57	1	137	II.C.2.a
117P-M-01	Primary Pt.	117	117P	6	67.77435	-163.62780	N	128	3	143	II.C.2.a
117R-M-01	Random Dupe	117	117R	6	67.7742	-163.62740	N	128	2	139	
118P-M-01	Primary Pt.	118	118P	6	67.64658	-164.12829	N	0	0	8	II.C.2.a
119P-M-01	Primary Pt.	119	119P	6	67.67003	-164.10435	N	0	0	14	II.C.2.f
119R-M-01	Random Dupe	119	119R	6	67.67029	-164.10558	N	0	0	15	
120P-M-01	Primary Pt.	120	120P	6	67.64358	-164.03293	N	310	1	35	II.C.2.a
121A-M-01	Auxillary Pt.	121	121A	6	67.68721	-163.96585	N	0	0	67	II.C.2.a
122A-M-01	Auxillary Pt.	122	122A	6	67.70433	-163.94925	N	0	0	54	II.B.2.a
122R-M-01	Random Dupe	122	122R	6	67.70469	-163.94901	N	0	0	55	
123P-M-01	Primary Pt.	123	123P	6	67.73133	-163.90724	N	240	2	66	II.C.2.a
124P-M-01	Primary Pt.	124	124P	6	67.7731	-163.86289	N	30	6	83	II.C.2.a
124R-M-01	Random Dupe	124	124R	6	67.77313	-163.86386	N	12	6	83	
125P-M-01	Primary Pt.	125	125P	6	67.76243	-163.77362	N	0	0	122	II.C.2.a
126P-M-01	Primary Pt.	126	126P	6	67.67938	-164.14578	N	0	0	20	II.C.2.a
127P-M-01	Primary Pt.	127	127P	6	67.71309	-164.13441	N	0	0	17	II.C.2.d
127R-M-01	Random Dupe	127	127R	6	67.71293	-164.13450	N	0	0	17	
136P-M-01	Primary Pt.	136	136P	7	67.08741	-163.10832	S	160	3	26	II.C.2.a
137P-M-01	Primary Pt.	137	137P	7	67.15244	-162.88026	S	82	6	86	II.C.1.a
138P-M-01	Primary Pt.	138	138P	7	67.23076	-163.21822	S	158	10	146	II.D.2.e
138R-M-01	Random Dupe	138	138R	7	67.23042	-163.21825	S	158	10	142	
139P-M-01	Primary Pt.	139	139P	7	67.22995	-163.36613	S	272	4	161	???
140A-M-01	Auxillary Pt.	140	140A	7	67.22334	-163.53589	S	80	15	87	II.C.2.a
140R-M-01	Random Dupe	140	140R	7	67.22353	-163.53590	S	80	15	87	
141A-M-01	Auxillary Pt.	141	141A	7	67.1564	-163.26288	S	206	11	140	II.D.1
141D-M-01	Field Dupe	141	141D	7	67.1564	-163.26288	S	206	11	140	II.D.1

Moss Code	Plot Type	Sample Point	Sample No.	Stratum	Latitude	Longitude	Side of Road	Aspect (deg)	Slope	Elev (m)	Viereck Veg type
141R-M-01	Random Dupe	141	141R	7	67.15583	-163.26311	S	206	11	140	
142P-M-01	Primary Pt.	142	142P	7	67.27891	-163.60470	S	163	8	78	II.C.2.a
142R-M-01	Random Dupe	142	142R	7	67.27878	-163.60371	S	163	8	70	
143P-M-01	Primary Pt.	143	143P	7	67.32898	-163.44505	S	261	6	93	II.C.2.a
144P-M-01	Primary Pt.	144	144P	7	67.45183	-163.32950	S	153	8	213	II.C.2.a
145P-M-01	Primary Pt.	145	145P	7	67.44043	-163.62465	S	126	4	52	II.C.2.a
145R-M-01	Random Dupe	145	145R	7	67.44031	-163.62530	S	98	4	50	
146P-M-01	Primary Pt.	146	146P	8	67.80471	-163.89112	N	260	2	86	II.C.2.a
146R-M-01	Random Dupe	146	146R	8	67.80461	-163.89174	N	260	2	85	
147A-M-01	Auxiliary Pt.	147	147A	8	67.86042	-163.83940	N	210	1	58	II.C.2.a
148D-M-01	Field Dupe	148	148D	8	67.92378	-163.95090	N	228	3	137	II.C.2.h
148P-M-01	Primary Pt.	148	148P	8	67.92378	-163.95090	N	228	3	137	II.C.2.h
148R-M-01	Random Dupe	148	148R	8	67.92402	-163.95037	N	228	3	137	
149P-M-01	Primary Pt.	149	149P	8	67.85516	-164.12459	N	340	5	85	II.C.2.a
150P-M-01	Primary Pt.	150	150P	8	67.81903	-164.29711	N	???	4	43	II.C.2.a
151P-M-01	Primary Pt.	151	151P	8	67.90621	-164.35265	N	120	4	70	II.C.2.a
151R-M-01	Random Dupe	151	151R	8	67.90602	-164.35270	N	124	4	69	
152P-M-01	Primary Pt.	152	152P	8	67.96435	-163.75231	N	0	0	138	II.C.2.a
153P-M-01	Primary Pt.	153	153P	8	68.10173	-164.17181	N	112	5	104	II.C.2.a
154P-M-01	Primary Pt.	154	154P	8	67.89215	-163.48068	N	360	3	91	II.C.2.a
155P-M-01	Primary Pt.	155	155P	8	68.10687	-163.96071	N	225	15	169	II.C.2.a
155R-M-01	Random Dupe	155	155R	8	68.1067	-163.96006	N	225	15	169	
156D-M-01	Field Dupe	156	156D	8	68.10796	-163.52817	N	90	25	263	II.C.1.b
156P-M-01	Primary Pt.	156	156P	8	68.10796	-163.52817	N	90	25	263	II.C.1.b
156R-M-01	Random Dupe	156	156R	8	68.10818	-163.52821	N	90	25	263	
157P-M-01	Primary Pt.	157	157P	8	67.94082	-164.59391	N	58	10	86	II.C.2.a
157R-M-01	Random Dupe	157	157R	8	67.94061	-164.59331	N	58	10	86	
159P-M-01	Primary Pt.	159	159P	8	68.21663	-164.26021	N	180	2	271	II.D.1.c
159R-M-01	Random Dupe	159	159R	8	68.21677	-164.26083	N	180	3	271	
160P-M-01	Primary Pt.	160	160P	8	68.13186	-164.46622	N	300	3	192	II.C.2.a
160R-M-01	Random Dupe	160	160R	8	68.1316	-164.46566	N	300	3	192	
161P-M-01	Primary Pt.	161	161P	5	67.58675	-163.95475	S	300	9	88	II.C.2.a
161R-M-01	Random Dupe	161	161R	5	67.58625	-163.95436	S	300	9	88	
162P-M-01	Primary Pt.	162	162P	5	67.57075	-163.95112	S	204	4	73	II.C.2.a
162R-M-01	Random Dupe	162	162R	5	67.5708	-163.95155	S	204	4	73	
163P-M-01	Primary Pt.	163	163P	5	67.55661	-163.94781	S	230	1	50	II.C.2.a
163R-M-01	Random Dupe	163	163R	5	67.55713	-163.94814	S	230	1	49	

Moss Code	Plot Type	Sample Point	Sample No.	Stratum	Latitude	Longitude	Side of Road	Aspect (deg)	Slope	Elev (m)	Viereck Veg type
164P-M-01	Primary Pt.	164	164P	5	67.54817	-163.98879	S	0	0	23	II.C.2.a
170P-M-01	Primary Pt.	170	170P	7	67.09547	-162.81079	S	311	2	48	II.C.2.a
170R-M-01	Random Dupe	170	170R	7	67.09599	-162.80917	S	311	2	50	
171P-M-01	Primary Pt.	171	171P	7	67.51963	-163.48752	S	99	20	161	II.C.2.c
201P-M-01	Off-grid	201	201O	0	67.72124	-163.60171	S	220	4	125	II.C.2.a
202P-M-01	Off-grid	202	202O	0	67.7398	-163.54627	S	72	2	168	II.C.2.a
203P-M-01	Off-grid	203	203O	0	67.73757	-163.54616	S	122	1	162	II.D.1.c